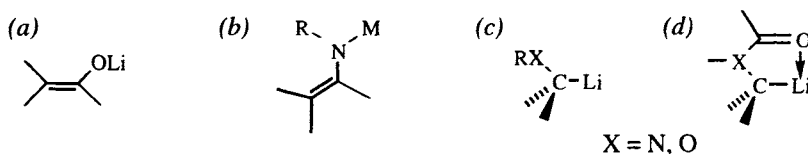


# Enolate, Azaenolate, and Organolithium Alkylations

Originally, the term ‘carbanion’ was used to refer to anionic reactive intermediates whose actual structure was rather poorly understood. In recent years, considerable advances have been made in developing the chemistry of carbanionic species and in understanding the structure of ‘carbanions,’ especially as regards the involvement of the metal [1-6]. In this chapter we will focus on three types of intermediate that fall into the category of ‘carbanion.’ Our discussion will be further limited to alkylations: carbon-carbon bond-forming reactions with electrophiles such as alkyl halides that produce only one stereocenter. Aldol and Michael additions are covered in Chapter 5, and reactions with heteroatom electrophiles that form carbon-oxygen or carbon-nitrogen bonds are discussed in Chapter 8.

Carbanions that have found use in asymmetric synthesis are stabilized by one or more substituents (Figure 3.1). By far the most common ‘carbanion stabilizing’ functional group is the carbonyl. Although early texts (*e.g.*, [7]) referred to the conjugate base of carbonyl compounds as carbanions, these species are now universally known as enolates (Figure 3.1a). Closely related to enolates are their nitrogen analogs, azaenolates (Figure 3.1b). As we will see, the fact that there is a substituent on the nitrogen is important to asymmetric synthesis because it provides a convenient foothold for attachment of a chiral auxiliary. In recent years, a new type of chiral ‘carbanion’ has emerged: organolithium species in which the carbon bearing the metal is stereogenic (Figure 3.1c,d). Again, the negative charge is stabilized in these species, but not by resonance as is the case with enolates and azaenolates. Instead, heteroatoms on the lithiated carbon provide inductive stabilization; in some instances chelation may be involved.



**Figure 3.1.** Enolates, azaenolates, and  $\alpha$ -heteroatom organolithiums.

## 3.1 Enolates and azaenolates<sup>1</sup>

The deprotonation of a carbonyl gives a nucleophilic species that reacts with electrophiles such as alkyl halides to afford products of substitution at the  $\alpha$  carbon. Because of this reactivity, the intermediate species used to be drawn with a negative

<sup>1</sup> For comprehensive coverage of enolate alkylations, see refs. [8,9].

charge on carbon (Figure 3.2a). Resonance considerations later suggested that the negative charge should be placed on the more electronegative oxygen (Figure 3.2b). When enolate reactions are carried out in aqueous or alcohol solution, the ionic species are separately solvated, and this type of representation is justified. Unfortunately, the same usage has persisted, even when the reactions are conducted in aprotic solvents where solvent-separated ions are not likely to exist. A more appropriate notation is to affix the metal to the oxygen (Figure 3.2c). Spectroscopic and X-ray data have revealed that metal enolates are usually (always?) aggregated, both in the solid state and in ethereal or hydrocarbon solution (Figure 3.2d). The illustrations in Figure 3.2 show the historical progression of these notations, which Seebach whimsically calls “the route of the sorcerer’s apprentice” [5].

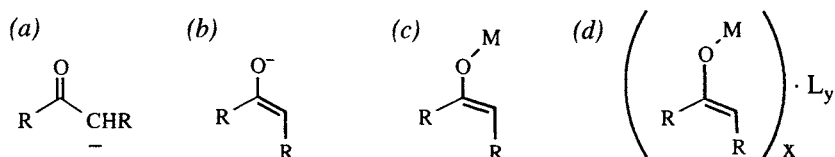
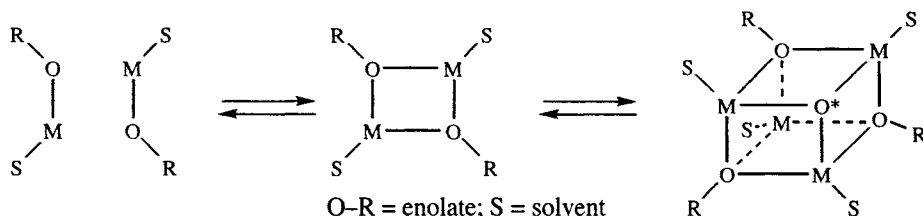


**Figure 3.2.** Various notations for an enolate, from a naked carbanion or enolate, via a metal enolate, to supramolecular aggregates (after ref. [5]).

Enolates may form supramolecular<sup>2</sup> species such as dimers, tetramers, or hexamers, and these species are often in equilibrium (Scheme 3.1). Enolates may also form mixed aggregates with added salts or with secondary or tertiary amines. The existence of such species has been proven in the solid state by X-ray crystallography, and colligative effects and NMR studies have confirmed their existence in solution (reviews: [5,6,8,12-14]; see also: [15-18]). Interestingly, dimers are even found in crystals of tetrabutylammonium malonates and cyanoacetates [19], indicating that a metal is not necessary for supramolecular organization!

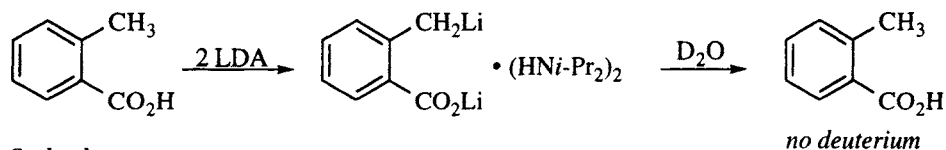


**Scheme 3.1.** Equilibrating dimeric and tetrameric enolate aggregates. Formal charges are not shown. There is probably more than one solvent molecule coordinated to the monomers (left) and dimer (middle). In the tetramer (right), the R moiety is deleted from the indicated oxygen (O\*) for clarity.

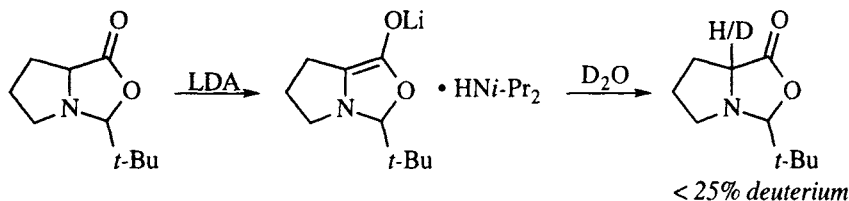
Chemical evidence also confirms the presence of supramolecular complexes in enolate reactions. For example, added salts can affect the product ratio of enolate alkylations [20-25]. Evidence of mixed aggregation between enolates and secondary amines includes experiments such as those illustrated in Scheme 3.2 where quench-

<sup>2</sup> The term supramolecular was coined by Lehn to refer to “organized entities ... that result from the association of two or more chemical species held together by intermolecular forces” [10,11].

Creger:



Seebach:



**Scheme 3.2.** Enolate-diisopropylamine complexes do not incorporate deuterium upon quenching with  $D_2O$ . (a) Creger demonstrated the phenomenon with *o*-toluic acid [26]. (b) Seebach showed that lactone enolates behave similarly [27].

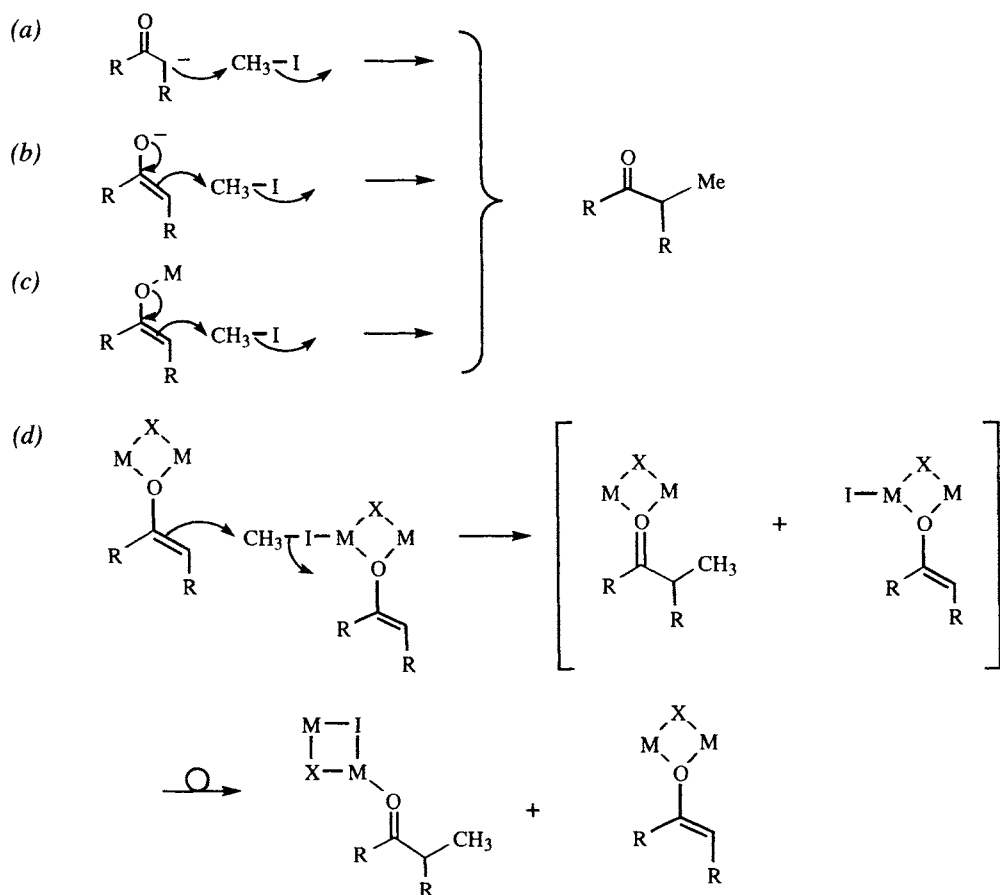
ing with  $D_2O$  or MeOD produces little or no deuterium incorporation, indicating that the enolate is protonated by the secondary amine from within a supramolecular aggregate [26,28–32].

The phrase “conducted tour mechanism” was coined by Cram to describe the removal of a proton by a base and its subsequent return to a different face of the same molecule from which it was removed [1]. Originally, the conducted tour mechanism was postulated to explain the observation that rates of racemization of deuterated carbon acids were faster than hydrogen-deuterium exchange in solutions of potassium *tert*-butoxide/*tert*-butyl alcohol. Thus, “the basic catalyst takes hydrogen or deuterium on a ‘conducted tour’ of the substrate from one face of the molecule to the [other]” (ref. [1], p. 101). This process was envisioned as a rotation of the carbanion within the solvent cage. We now recognize that the secondary amine forms a mixed aggregate with the enolate, such that the reprotonation (and perhaps conformational motion) is ‘intramolecular.’

A complete understanding of enolate chemistry must include knowledge of the aggregation of the enolate species involved [5]. Consider the reaction of an enolate with an alkyl halide as it may have been depicted over the years (Scheme 3.3), progressing from the simple carbanion alkylation to the reaction of supramolecular aggregates.

The mechanism depicted in Scheme 3.3d may be the closest to reality for the reaction of an enolate with an alkyl halide, but this picture is dependent on the individual system under study. For our purposes, we can rationalize most enolate reactions by considering metal enolates as monomers (as in Scheme 3.3c), while realizing that the other coordination sites of the metal may be occupied by ligands that may be solvent molecules, additives such as HMPA, DMPU or TMEDA,<sup>3</sup>

<sup>3</sup> HMPA: hexamethylphosphoramide. DMPU: *N,N'*-dimethylpropyleneurea. TMEDA: tetramethylethylenediamine. Both are additives that coordinate metals and may inhibit aggregation. Note that mechanistic interpretation of the effect of additives, especially TMEDA in THF solvent, are risky [33].



**Scheme 3.3** Alkylation of an “enolate” (a) naked carbanion; (b) naked enolate; (c) metal enolate; (d) supramolecular alkylation and rearrangement (after ref. [5]).

anions of added salts, or another molecule of enolate. The interested reader is referred to Seebach’s review to see the types of supramolecular complexes that may arise in the chemistry of lithium enolates [5].

### 3.1.1 Deprotonation of carbonyls<sup>4</sup>

A number of bases may be used for deprotonation, but the most important ones are lithium amide bases such as those illustrated in Figure 3.3.<sup>5</sup> Although other alkali metals may be used with these amides, lithium is the most common. Amide bases efficiently deprotonate virtually all carbonyl compounds, and do so regioselectively with cyclic ketones such as 2-methylcyclohexanone (*i.e.*,  $\text{C}_2$  vs.  $\text{C}_6$  deprotonation) and stereoselectively with acyclic carbonyls (*i.e.*,  $E(O)$ - vs.  $Z(O)$ -<sup>6</sup> enolates). If the carbonyl is added to a solution of the lithium amide, deprotonations are irreversible and kinetically controlled [36–38]. Under such conditions, the con-

<sup>4</sup> For a review on enolate formation, see ref. [34].

<sup>5</sup> LDA is stable in both ether and THF at room temperature for 24 hours, but that LTMP has a half-life of 12 hours in THF and only 4 hours in ether at room temperature [35].

<sup>6</sup> See glossary, section 1.6, for the definition of the  $E(O)/Z(O)$  descriptors of enolate geometry.

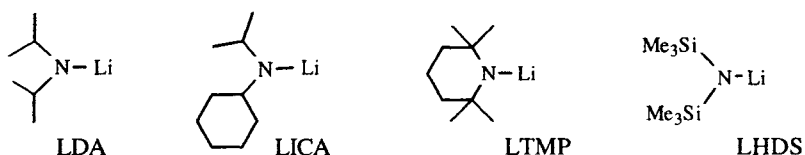
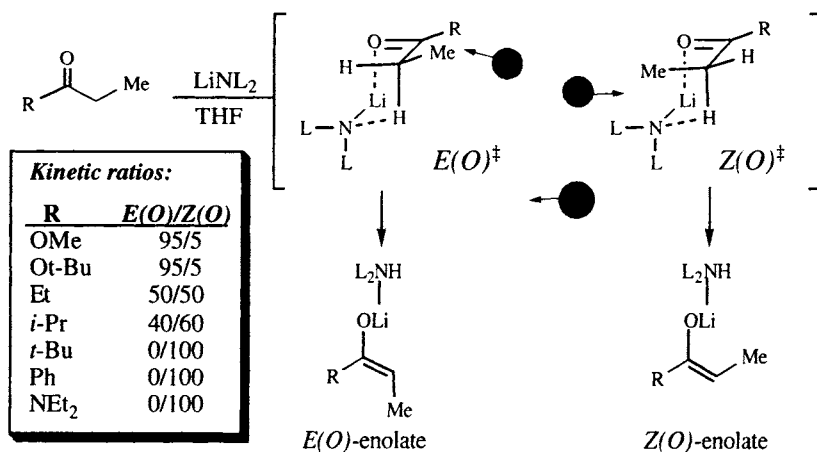


**Figure 3.3.** LDA = lithium diisopropyl amide, LICA = lithium isopropyl cyclohexyl amide, LTMP = lithium tetramethylpiperidide, LHDS = lithium hexamethyldisilyl amide.

figuration of an acyclic enolate is determined during the deprotonation step, and subsequent isomerization is probably not important [38]. The most commonly cited deprotonation model has the lithium amide base and the carbonyl reacting in a cyclic, 6-membered transition state such that the  $\alpha$ -proton and the metal are transferred simultaneously [39]. This mechanism, proposed by Ireland in 1976, may be used to explain the preferred formation of  $E(O)$ - or  $Z(O)$ -enolates of acyclic esters, ketones and amides [14], at least in the absence of coordinating additives such as HMPA (*vide infra*). As shown in Scheme 3.4, the transition states for the deprotonation to the  $E(O)$ - and  $Z(O)$ -enolates are apparently controlled by a balance of 1,2-eclipsing interactions between the  $\alpha$ -methyl group and the carbonyl substituent, R, and 1,3-diaxial interactions between the nitrogen ligand and  $\alpha$ -methyl. For esters, the atom attached to the carbonyl is oxygen, and the alkyl group (even one as large as a *tert*-butyl) can rotate away from the  $\alpha$ -methyl and have no effect on enolate geometry. In such cases,  $E(O)^\ddagger$  is more stable than the  $Z(O)^\ddagger$  due to the 1,3-diaxial interaction of the nitrogen ligand and the  $\alpha$ -methyl in the latter. As the steric requirements of the carbonyl substituent increase, especially in the plane of the forming double bond, van der Waals repulsion increases the  $A^{1,3}$  strain in the enolate and  $E(O)^\ddagger$  is destabilized relative to  $Z(O)^\ddagger$ . Thus, for large substituents such as *tert*-butyl, and for substituents such as phenyl or dialkylamides that are coplanar with the carbonyl, the  $Z(O)$ -enolate is formed exclusively. Molecular mechanics calculations confirm the general validity of these arguments [40].

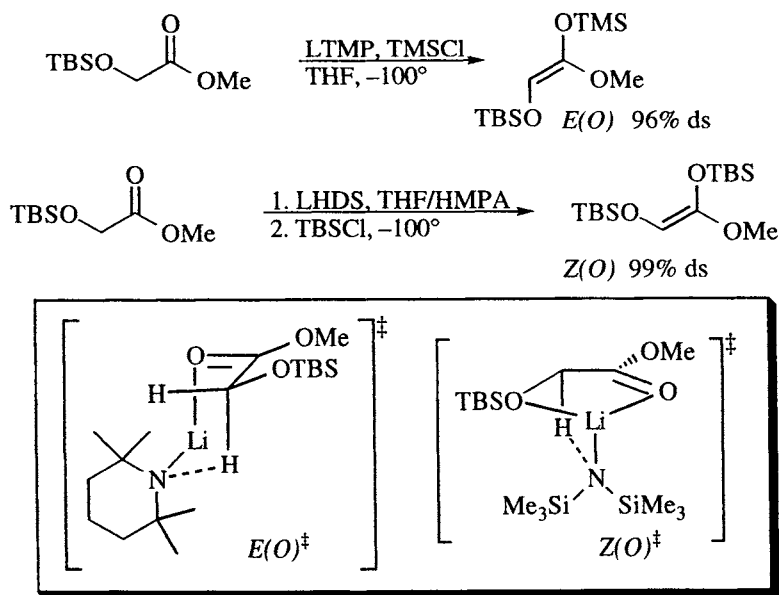


**Scheme 3.4.** Ireland model [39] transition structures for the deprotonation of acyclic carbonyls (after ref. [14]). The gray circles point out the sources of strain in the transition states:  $A^{1,3}$  strain increasing as the enolate develops in  $E(O)^\ddagger$  and 1,3-diaxial strain in  $Z(O)^\ddagger$ . For structural information from X-ray data, see ref. [29].

In the presence of coordinating additives such as HMPA, DMPU or TMEDA, the trend outlined in Scheme 3.4 may not hold [36,41-43]. For example, in the presence of HMPA, LDA deprotonation of 3-pentanone affords a 5:95 mixture of *E(O)*- and *Z(O)*-enolates under conditions of thermodynamic control (equilibration by reversible aldol addition) [39,41], but a 50:50 mixture under kinetic control [41,42].

For esters, thermodynamic equilibration of enolates is less likely, but additives can still affect the selectivity. Using LDA in THF for example, deprotonation of ethyl propionate is 94% *E(O)*-selective, but in THF containing 45% DMPU, deprotonation is 93-98% *Z(O)*-selective [36]. Ireland rationalizes this observation in terms of the transition states in Scheme 3.4 as follows: in the absence of additives, there is a close interaction between the metal, the carbonyl oxygen and the base which leads to a tight transition structure and *E(O)*<sup>‡</sup> is favored. In the presence of coordinating additives, there is more effective solvation for the lithium, and therefore weakened interaction between the lithium and the carbonyl oxygen. The cyclic transition structures will be expanded, and may even open to an acyclic transition structure. When the association between the base and the ester is diminished, the 1,3-diaxial strain in *Z(O)*<sup>‡</sup> is reduced, whereas *E(O)*<sup>‡</sup> (and acyclic structures with similar torsion angles) are still destabilized by A<sup>1,3</sup> strain [36].

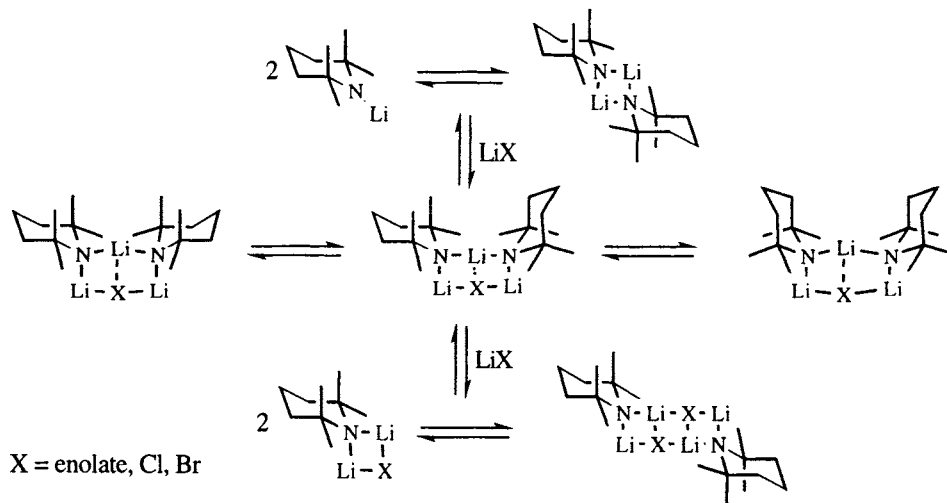
For  $\alpha$ -silyloxyacetates, Yamamoto reported the selective deprotonations shown in Scheme 3.5. These examples are consistent with the trend noted by Ireland, in that HMPA favors formation of the *Z(O)*-enolate, but other factors may also be involved. In fact, the transition structures proposed by Yamamoto (Scheme 3.5, inset) invoke chelation by the silyloxy group in one instance but not the other. Note however, that the Ireland argument could also be applied here: with LTMP as the



**Scheme 3.5.** Selective formation of either *E(O)*- or *Z(O)*-enolates of silyloxyacetates [43]. *Inset:* The authors suggest that the *E(O)*-enolate is formed according to the Ireland rationale (Scheme 3.4), but that the *Z(O)*-enolate is formed by chelation in the transition state.

base, the  $Z(O)^{\ddagger}$  Ireland transition structure (Scheme 3.4) would be destabilized considerably by 1,3-diaxial interactions between the silyloxy and the bulky tetramethylpiperidine. With LHDS in THF/HMPA, the lithium would be solvated by the HMPA, and the 1,3-diaxial interactions would be attenuated as explained above, but they could also be diminished because of the longer Si–N bond distance (compared to C–N) in the amide. Independent of mechanism, *the bottom line is that both ester  $E(O)$ - and  $Z(O)$ -enolates can be produced selectively.*

The Ireland rationale also fails to account for phenomena such as changes in selectivity as the reaction proceeds and for the effect of added lithium salts. For example, the deprotonation of 3-pentanone by LTMP affords a 97:3  $E(O)/Z(O)$  selectivity at 5% conversion, but <90:10 selectivity at  $\geq 80\%$  conversion [38]. Moreover, the presence of 0.3–0.4 equivalents of lithium chloride or  $\geq 1.0$  equivalents of lithium bromide enhance the  $E(O)/Z(O)$  selectivity (at complete conversion) to 98:2.<sup>7,8</sup> LTMP is one of the most sterically hindered lithium amides known, and there is some evidence that the formation of mixed aggregates is sterically driven: mixed dimerization with sterically unhindered LiX species provides a simple means to alleviate the steric demands of LTMP aggregates (Scheme 3.6). For example, a 50:50 mixture of cyclohexanone enolate and LTMP shows significant heterogeneous aggregation, whereas a similar mixture with LDA shows <5% mixed dimer [44]. The observation of decreased selectivity as enolate accumulates or with added lithium halide [38], as well as the observation of equilibrating mixed aggregates of LTMP, lithium enolates, and lithium halides [44] led to the conclusion that lithium salt dependent selectivities stem from the intervention of mixed aggregates in the



**Scheme 3.6.** Proposed dynamic equilibria of LTMP and added lithium salts (after ref. [44]).

- <sup>7</sup> For a simple protocol for the preparation of LTMP/LiBr solutions by deprotonation of TMP·HBr with butyllithium, which affords a 50:1 ratio of the  $E(O)$  and  $Z(O)$  enolates of 3-pentanone, see ref. [38].
- <sup>8</sup> Curiously, the presence of  $\geq 1.0$  equivalents of lithium chloride leaves the  $E(O)/Z(O)$  ratio unchanged from the ratio in the absence of lithium halide [38].

product determining transition state(s) [38]. Lithium bis(2-adamantyl)amide, which is even more hindered than LTMP, forms mixed aggregates with ketone enolates but not with lithium halides, and enolizes ketones with a very high degree of  $E(O)/Z(O)$  selectivity [17]. The  $E(O)/Z(O)$  ratio of ketone enolates is also dependent on the amount of hexane in the THF solvent [45].

In light of the anomalies described above, it is apparent that the Ireland model is an oversimplification, but a clearer picture has not yet emerged. Indeed, expecting such a simple model to account for kinetic selectivities in a number of solvent systems with a variety of carbonyl substrates and amide bases is asking a lot. There is some evidence that an 8-membered ring transition structure may be involved (deprotonation by a lithium amide 'open dimer'), and computational studies indicate that neither 6- nor 8-membered ring transition structures bear much resemblance to carbocyclic 6- or 8-membered rings. For a detailed discussion of these issues, see ref. [46].

### 3.1.2 The transition state for enolate alkylations

The earliest work on the origin of stereoselectivity of enol and enolate reactions was done some forty years ago in the steroid arena [47,48], at the beginning of the modern era of stereochemistry. More recent efforts have focussed on the stereoelectronic effects exerted by the frontier orbitals on the trajectory of electrophilic attack [49]. Specifically, Agami suggested that the approach trajectory for the electrophile should be as shown in Figure 3.4a and b [50-52]. Using *ab initio* methods, Houk found a transition structure for the alkylation of acetaldehyde enolate with methyl fluoride which agreed with Agami's prediction of Figure 3.4a. An 'out of perpendicular' component (*à la* Figure 3.4b) was not found, but the methyl fluoride transition state is late relative to methyl iodide, and a structure associated with an earlier transition state (less bond making between nucleophile and electrophile) would probably exhibit this feature [53]. Note the pyramidalization of the  $\alpha$ -carbon in Houk's transition structure, a feature that crops up in a number of calculated transition structures [54,55] and which appears to be important in other reaction types as well [29,56]. Often, pyramidal  $sp^2$  atoms are found in X-ray crystal structure structures of ground state reactants such as enones.<sup>9</sup>

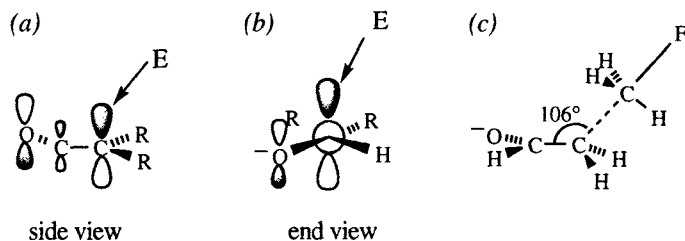
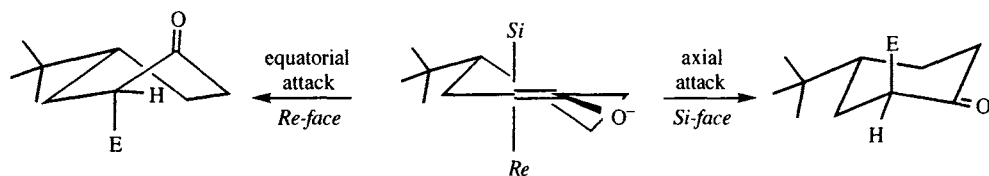


**Figure 3.4.** Theoretical approach trajectories (drawn in the plane of the paper) for electrophilic attack at an enolate carbon. (a) and (b) Agami's trajectory [50-52]; (c) Houk's trajectory [53].

<sup>9</sup> See the discussion in Section 4.4.3 (Figure 4.23) for a discussion of the phenomenon of pyramidalization in nucleophilic additions to trigonal atoms.



Studies on the stereoselective alkylation of conformationally rigid cyclohexanone enolates (summarized in ref. [14]) indicate that the transition state is early. In these systems, axial attack affords a product in a chair conformation while equatorial attack affords a twist-boat (Scheme 3.7). If the relative stability of these conformers were felt in the transition state, significant selectivity would ensue. However the low selectivities observed (55:45 for the reaction of the lithium enolate of 4-*tert*-butylcyclohexanone with methyl iodide [57]) suggest an early transition state according to the Hammond postulate. Somewhat higher selectivity for axial deuteration [57] is consistent with a less exothermic reaction. A higher propensity for axial alkylation (70:30) with a tetrabutylammonium cation [58] or when the *tert*-butyl group is in the 3-position (80:20) suggest that other factors (aggregation?) are also at work.



**Scheme 3.7.** Equatorial and axial approach of an electrophile to a cyclohexanone.

Stereocenters at the  $\beta$ -position can have an important effect on the differentiation of the enolate faces. The conformation of the 2-3 (allylic) bond of an acyclic enolate is governed primarily by  $A^{1,3}$  strain (see glossary, section 1.6, and ref. [59]) such that the most stable conformation has the smallest substituent eclipsing the double bond, independent of enolate geometry (Figure 3.5).

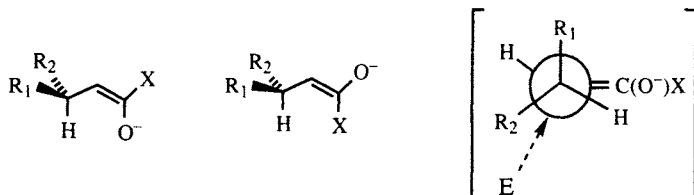
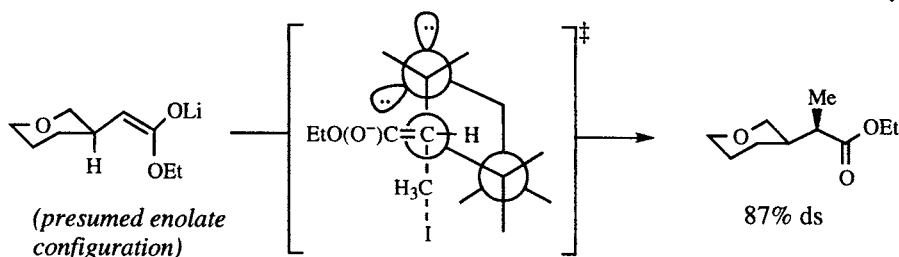


**Figure 3.5.** Ground state (left and center) and transition state conformations of  $\beta$ -substituted enolates.

In the transition state, the  $\alpha$ -carbon is pyramidalized, and the substituents on the  $\beta$ -carbon are rotated such that the substituent that is the better  $\sigma$ -donor is perpendicular to the double bond [55,60,61]. The opposite face is then preferred by the approaching electrophile, as shown on the right in Figure 3.5. This ‘antiperiplanar effect’ is a phenomenon that occurs quite often in organic chemistry,<sup>10</sup> and arises because of the favorable overlap of an allylic  $\sigma$ -bond with the  $\pi$ -orbital of the enolate. The resulting perturbation raises the energy of the enolate HOMO and renders it more reactive [61]. For substituents ( $R_1$  and  $R_2$ , Figure 3.5) that differ only in steric bulk, the selectivity is small (65:35), but the example in Scheme 3.8 illustrates how the electronic effect of an alkoxy substituent can profoundly influence face selectivity by proper alignment of its lone pairs.

<sup>10</sup> Another type is the Felkin-Anh descendant of Cram’s rule, which is discussed in detail in Chapter 4 (Section 4.1).

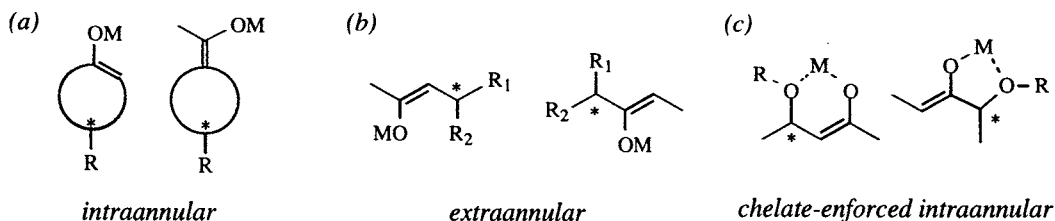


**Scheme 3.8.** Stereoselective alkylation of an ester enolate determined solely by stereoelectronic effects [61].

### 3.1.3 Enolate and azaenolate alkylations

In Section 1.3 (pp. 4-7), the relationship of extant chirality in a reacting system to any newly created stereocenters was categorized according to the relationship of the former and the latter in a metal complex in the transition state. Thus, *intraligand* asymmetric induction occurs when both the “old” and the “new” stereocenters are on the same ligand of the metal, and *interligand* asymmetric induction occurs when the existing stereocenters are on another ligand. Evans [14] had grouped chiral enolate systems into three categories, based on the location of the existing stereocenter relative to any rings present (intrannular if it is within a ring and extrannular if it is not). In the present context, these categories are sub-classes of intraligand asymmetric induction, as shown in Figure 3.6: *intraannular*, in which the existing stereocenter is contained in a ring that is bonded to the enolate at two points, *extraannular*, in which the moiety containing the stereocenter is bonded to the enolate at one point, or *chelate-enforced intraannular*, in which the stereocenter is contained in a chelate ring containing the enolate metal.

#### *Intraligand asymmetric induction*



#### *Interligand asymmetric induction*

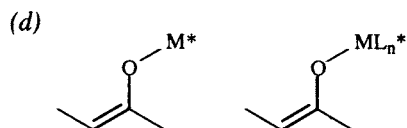


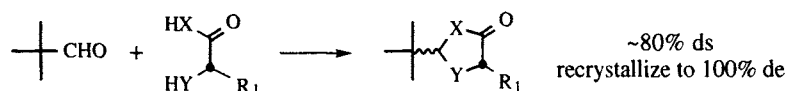
**Figure 3.6.** Two categories of asymmetric induction are intraligand (a-c) and interligand (d). The former may be subdivided [14] into (a) intraannular; (b) extraannular; and (c) chelate-enforced intraannular.

The widespread use of enolate alkylations for carbon-carbon bond formation has led to the development of a large number of methods for asymmetric synthesis, and

the search goes on. The following discussion is intended to highlight enolate alkylation methods that seem to have broad applicability or which illustrate one of the categories mentioned above.

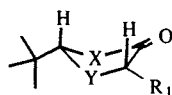
**Intraligand asymmetric induction.** An instructive introduction to intraannular alkylations is the ‘self-regeneration of chirality centers’ concept introduced by Seebach [62-66]. Scheme 3.9 illustrates the concept and Table 3.1 lists several representative examples. A chiral educt, such as an amino acid derivative, is condensed with pivaldehyde. This derivatization creates a new stereocenter selectively, and this second stereocenter then controls the selectivity of the subsequent alkylation by directing the electrophile to the face of the enolate opposite the *tert*-butyl group, a good example of intraannular 1,3-asymmetric induction. After purification of the alkylation product, hydrolysis affords enantiomerically pure products.

(a) Introduction of the ‘achiral’ auxiliary:



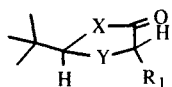
Puckered conformation, *cis* favored:

X, Y = S, O

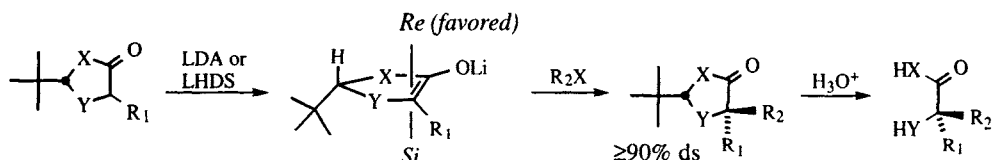


Planar conformation, *trans* favored:

X, Y = NHAc



(b) Asymmetric alkylation and auxiliary removal:



**Scheme 3.9.** Self-regeneration of chirality centers [62-66].

**Table 3.1.** Selected examples of Seebach's “self-regeneration” of chirality centers (Scheme 3.9).

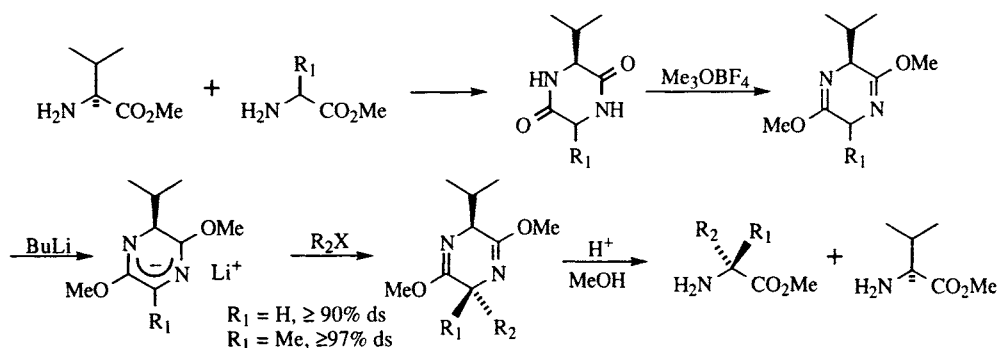
X/Y	R <sub>1</sub> /R <sub>2</sub>	dr <sup>1</sup>	% Yield	Reference
O/O	Me/Et	94:6	82	[62]
O/O	Ph/ <i>n</i> -Pr	90:10	84	[62]
O/S	Me/allyl	>96:4	92	[62]
O/NCOPh	Me/Bn	>96:4	93	[64]
O/NCOPh	Bn/Me	>96:4	88	[64]
O/NCOPh	<i>i</i> -Pr/Me	100:0	53	[64]
MeN/NCOPh	Me/Et	>90:10	90	[65]
MeN/NCOPh	Me/Bn	>90:10	73	[65]
MeN/NBOC <sup>2</sup>	H/Bn	100:0	64	[63]
MeN/NBOC <sup>2</sup>	H/allyl	100:0	85	[63]
MeN/Cbz <sup>2</sup>	H/ <i>i</i> -Pr	100:0	59	[63]

<sup>1</sup> Diastereomer ratio after purification.

<sup>2</sup> Obtained enantiomerically pure by resolution.

The concept of self-regeneration has been employed by other groups. For example, Vedejs has shown that condensation of a formamidino amino acid sodium salt with  $\text{PhBF}_2$  affords a mixture of oxazaborolidine diastereomers that are enriched in one isomer by an asymmetric transformation of the second kind.<sup>11</sup> Recrystallization gives the pure diastereomer shown in Scheme 3.10a. Deprotonation and alkylation is highly diastereoselective, with alkylation occurring preferentially on the *Si* face, trans to the *B*-phenyl group. The major product can be separated from its diastereomer by crystallization and/or chromatography. Removal of the boron and formamidino groups then give the enantiopure quaternary amino acid in

piperazine, one of which serves as the chiral auxiliary for  $\alpha$ -alkylation of the other. *O*-Alkylation gives the bis-lactim ether shown at the top right of Scheme 3.11. After deprotonation, alkylation occurs stereoselectively such that the electrophile approaches the anion anti to the isopropyl. Typical selectivities for this process are listed in Table 3.2. Advantages of this process are that selectivities are high and that it makes chiral quaternary carbons. Disadvantages are that the electrophiles must often be activated (*i.e.*, allylic, benzylic), and that the alkylated amino ester and the amino ester chiral auxiliary must be separated at the end.



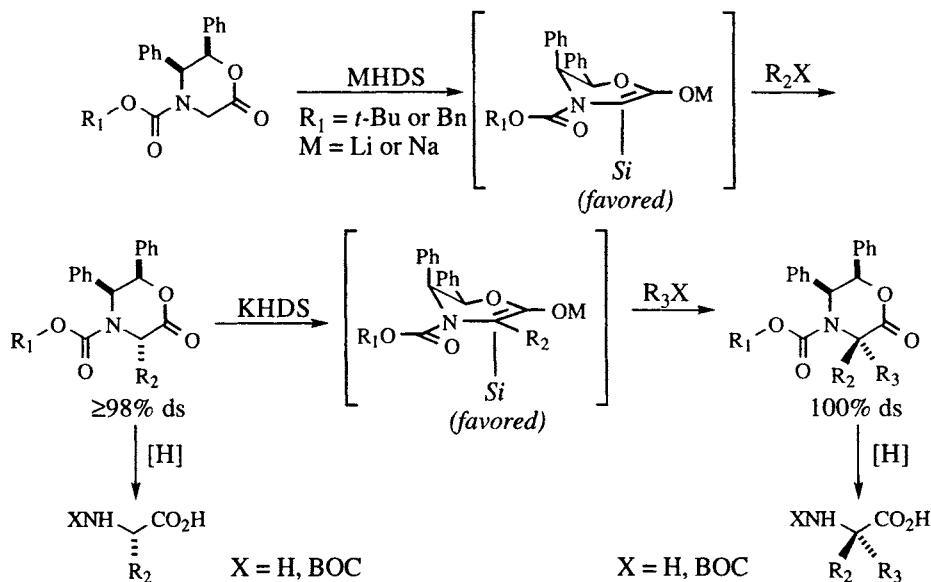
**Scheme 3.11.** Shöllkopf's bis-lactim ether amino acid synthesis [70].

**Table 3.2.** Examples of Shöllkopf's amino acid synthesis (Scheme 3.11 [70]).

$\text{R}_1/\text{R}_2$	% ds	% Yield
H/Bn	96	81
H/PhCH=CHCH <sub>2</sub>	97.5	90
H/ <i>n</i> -C <sub>7</sub> H <sub>15</sub>	87	62
Me/Bn	98	68
Me/PhCH=CHCH <sub>2</sub>	98	89
Me/ <i>n</i> -C <sub>7</sub> H <sub>15</sub>	98	43

A second method for amino acid synthesis was developed by Williams [71]. As shown in Scheme 3.12, the chiral diphenyloxazinone may be alkylated using LHDS or NHDS with excellent diastereoselectivity provided the alkylating agent is activated, such as a benzyl, allyl, or methyl halide. The stereoselectivity is  $\geq 98\%$  and the conformation shown in Scheme 3.12 was postulated to explain the selectivity. After the first alkylation, a second alkylation may be executed. After purification of the crystalline oxazinones, reductive cleavage of the benzylic-heteroatom bonds liberates the amino acid. This destruction of the "auxiliary" is a drawback to this strategy because of the high cost of the amino alcohol ( $>\$15/\text{g}$ ). Selected examples of this process are listed in Table 3.3. As with the Schöllkopf method, the electrophiles must be activated. However, in this self-immolative method the separation of the amino acid from the remainder of the auxiliary is not a complicating factor.

Another method for asymmetric alkylation of a masked glycine was reported by Yamada, and is shown in Scheme 3.13 [72]. In this example of a chiral glycine enolate, the Schiff base of *tert*-butyl glycine and an  $\alpha$ -pinene-derived ketone is delithiated with two equivalents of LDA. Presumably, the lithium alkoxide is chelat-



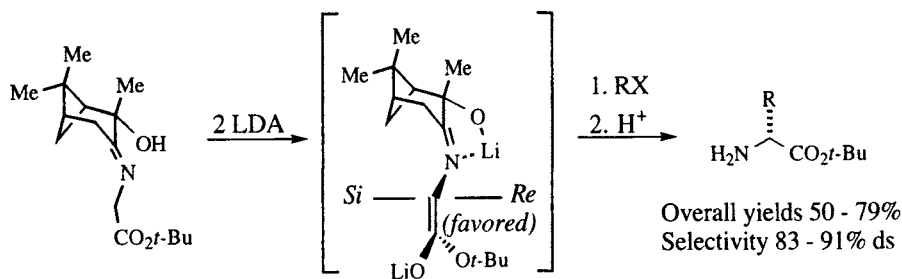
**Scheme 3.12.** William's oxazinone enolate amino acid synthesis [71]. The conformation shown in the two bracketed structures has the C-5 phenyl in the axial position to avoid A<sup>1,3</sup> interactions with the adjacent *N*-acyl group.

**Table 3.3.** Examples of Williams's amino acid synthesis (Scheme 3.12 [71]). In all cases, the diastereoselectivity was  $\geq 98\%$ .

R <sub>1</sub>	R <sub>2</sub>	R <sub>3</sub>	Base	% Yield (alkylation)	% Yield (amino acid)	% ee
<i>t</i> -Bu	allyl	-	LHDS	86	50-70	98
<i>t</i> -Bu	Me	-	NHDS	91	54	97
<i>t</i> -Bu	Bn	-	NHDS	70	76	98
Bn	Bn	-	NHDS	77	93	>99
<i>t</i> -Bu	Me	allyl	KHDS <sup>1</sup>	87 <sup>1</sup>	70	100
<i>t</i> -Bu	Me	Bn	KHDS <sup>1</sup>	84 <sup>1</sup>	93	100
<i>t</i> -Bu	<i>n</i> -Pr	allyl	KHDS <sup>1</sup>	90 <sup>1</sup>	60	100
Bn	Me	Bn	KHDS <sup>1</sup>	84 <sup>1</sup>	93	100

<sup>1</sup> Second alkylation.

ed to the nitrogen as shown. This tricyclic chelate is rigid and the dienolate must adopt the *s*-trans conformation in order to avoid severe nonbonding interactions with the  $\alpha$ -pinene moiety. Nonbonding interactions that restrict conformational motion are necessary for high selectivity in examples of extraannular asymmetric induction (Figure 3.6) such as these. Approach of the electrophile from the *Re* face gives the configuration shown. Although the authors did not determine the configuration of the enolate, if we assume that the enolate is *E*(*O*) as shown, then the Agami approach trajectory (Figure 3.4) would be slanted towards the back of the figure, trans to the alkoxide. Approach from the *Si* face would not only be on the concave face of the structure but would also be slanted back towards the  $\alpha$ -pinene moiety. Table 3.4 summarizes the selectivities reported for this asymmetric amino acid synthesis.



**Scheme 3.13.** Yamada's chiral glycine enolate [72].

**Table 3.4.** Stereoselective alkylations of Yamada's glycine enolate (Scheme 3.13) [72].

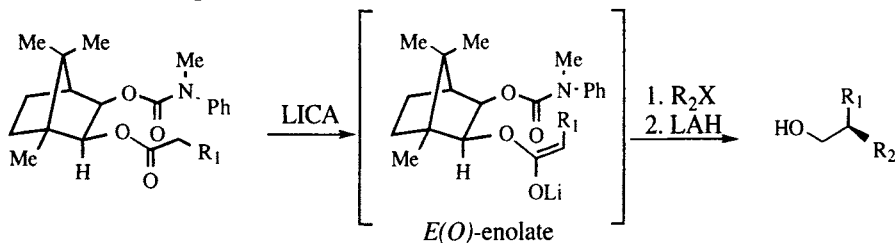
R	(presumed) % ds <sup>1</sup>	Yield <sup>2</sup>
Me	91	52
<i>i</i> -Bu	91	50
Bn	86	79
3,4-(MeO) <sub>2</sub> -C <sub>6</sub> H <sub>3</sub> CH <sub>2</sub>	83	62

<sup>1</sup> Calculated from %ee of product.

<sup>2</sup> Overall yield of amino acid ester.

During the 1980s, one of the major thrusts of asymmetric synthesis was the development of chiral auxiliaries for the alkylation and aldol addition of propionates. The following paragraphs describe some of the methods that evolved, beginning with two examples of propionate ester alkylations developed by Helmchen using chiral alcohols as the auxiliary and ending with propionic imide auxiliaries developed by Evans and Oppolzer.

The two ester enolate alkylation methods developed by Helmchen are illustrated in Schemes 3.14 and 3.15 [73-76]. These esters are designed so that one face of the enolate will be completely shielded by a second ligand appended to the camphor nucleus. As shown in Scheme 3.14, deprotonation by LICA affords the *E(O)*-enolate illustrated. Nonbonding steric interactions are thought to hold this enolate in the illustrated geometry.<sup>12</sup> Specifically, the OLi is thought to be syn to the illustrated endo carbinol hydrogen, since other rotamers would engender strain between various parts of the enolate and the camphor nucleus. Similarly, the most stable conformation of the carbamate shielding group has the endo C-H syn to the C=O. In this conformation, approach of the electrophile is only possible from the front (*Re*) face. After purification, LAH reduction affords enantiomerically pure alcohols as shown [73,74]. Representative examples of this procedure are listed in Table 3.5.



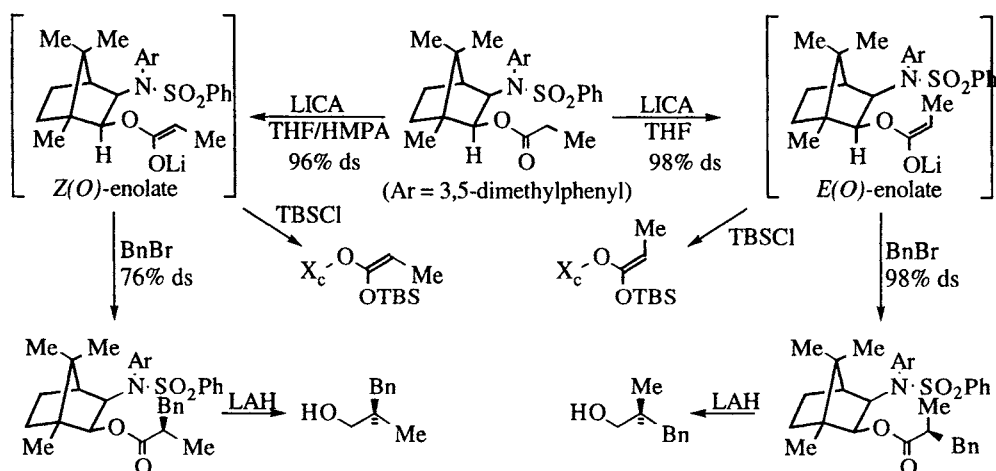
**Scheme 3.14.** Helmchen's asymmetric ester enolate alkylation [73,74].

<sup>12</sup> Note the similarity to the enolate conformations in Figure 3.6.

**Table 3.5.** Stereoselective alkylation of camphor ester enolates (Scheme 3.14).

R <sub>1</sub>	R <sub>2</sub>	Yield	%ds	Reference
Me	<i>n</i> -C <sub>16</sub> H <sub>33</sub>	83%	93	[73]
<i>n</i> -C <sub>16</sub> H <sub>33</sub>	Me	80%	90	[73]
Me	Bn	96%	94	[74]
Bn	Me	95%	95	[74]

Scheme 3.15 illustrates a different auxiliary derived from camphor, and which has similar design features, but which affords higher diastereoselectivity [75]. Additionally, Scheme 3.15 illustrates the selective formation of either an *E*(*O*)- or *Z*(*O*)-enolate based on the presence or absence of HMPA in the reaction mixture. Thus, deprotonation of the ester with LICA is 98% selective for the *E*(*O*)-enolate and deprotonation in the presence of HMPA is 96% selective for the *Z*(*O*)-enolate. Alkylation with benzyl bromide is more selective for the *E*(*O*)-enolate than for the *Z*(*O*), but after diastereomer separation, reduction gives enantiomerically pure *R*- or *S*-2-methyl-3-phenylpropanol, opposite enantiomers from the same auxiliary [75].

**Scheme 3.15.** Controlled stereoselective enolate formation and asymmetric alkylation of a "second generation" camphor ester enolate chiral auxiliary [75].

The mechanistic rationale for the selectivity of these ester enolate alkylations may be summarized as follows (Scheme 3.14 and 3.13 [74]):

- 1 Deprotonation in THF solvent gives *E*(*O*)-enolates while enolization in



Although accounting for the gross data, this rationale is not completely satisfactory. Subsequent studies [75] showed that addition of HMPA *after enolate formation but before electrophile addition* also had an effect on the selectivity of the alkylation, leading Helmchen to speculate that the sulfonamide in Scheme 3.15 (or presumably the urethane in Scheme 3.14) may be chelated to the lithium. Another possibility may be that the enolates are aggregated, and the effect of HMPA is to disrupt the aggregation. Additionally, the difference in selectivity between the *E(O)*- and *Z(O)*-enolate alkylations (Scheme 3.15) remains unexplained.

Helmchen has used this methodology in asymmetric synthesis of the three stereoisomers of the tsetse fly pheromone [73] and the side chain of  $\alpha$ -tocopherol [76], illustrated in Figure 3.7.

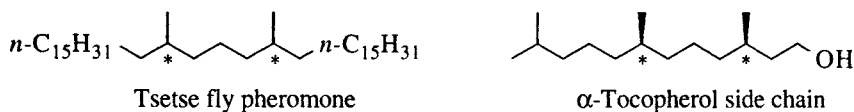
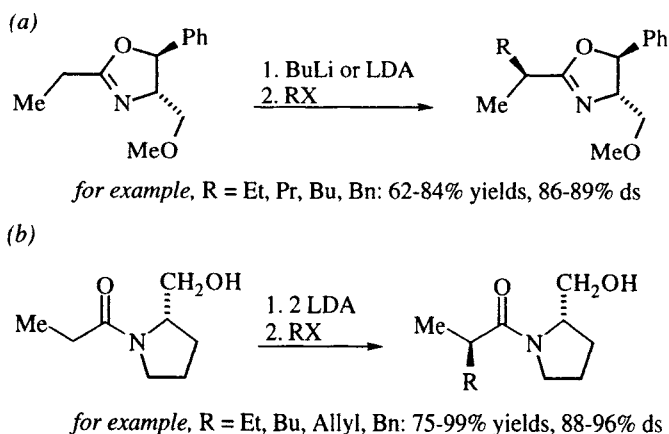


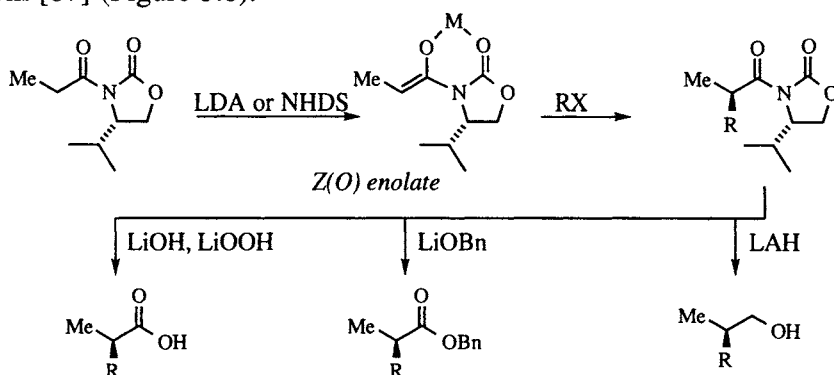
**Figure 3.7.** Natural products synthesized using Helmchen's ester enolates: the tsetse fly pheromone [73] and the side chain of  $\alpha$ -tocopherol [76].

It is generally true that restrictions on conformational mobility minimize the number of competing transition states and simplify analysis of the factors that affect selectivity. Chelation of a metal by a heteroatom often provides such restriction and also often places the stereocenter of a chiral auxiliary in close proximity to the  $\alpha$ -carbon of an enolate. This proximity often results in very high levels of asymmetric induction. A number of auxiliaries have been developed for the asymmetric alkylation of carboxylic acid derivatives using chelate-enforced intraannular asymmetric induction. The first practical method for asymmetric alkylation of carboxylic acid derivatives utilized oxazolines and was developed by the Meyers group in the 1970's (Scheme 3.16a), whose efforts established the importance and potential for chelation-induced rigidity in asymmetric induction (reviews: [77-79]). In 1980, Sonnet [80] and Evans [81,82] independently reported that the dianions of prolinol amides afford more highly selective asymmetric alkylations (Scheme 3.16b).



**Scheme 3.16.** Early examples of asymmetric enolate alkylations: (a) Meyers's oxazolines [77-79]; (b) Evans's [81,82] and Sonnet's [80] proline amide alkylations.

In 1982, Evans reported that the alkylation of oxazolidinone imides appeared to be superior to either oxazolines or prolinol amides from a practical standpoint, since they are significantly easier to cleave [83]. As shown in Scheme 3.17, enolate formation is at least 99% stereoselective for the *Z(O)*-enolate, which is chelated to the oxazolidinone carbonyl oxygen as shown. From this intermediate, approach of the electrophile is favored from the *Si* face to give the monoalkylated acyl oxazolidinone as shown. Table 3.6 lists several examples of this process. As can be seen from the last entry in the table, alkylation with unactivated alkyl halides is less efficient, and this low nucleophilicity is the primary weakness of this method. Following alkylation, the chiral auxiliary may be removed by lithium hydroxide or hydroperoxide hydrolysis [84], lithium benzyloxide transesterification, or LAH reduction [85]. Evans has used this methodology in several total syntheses. One of the earliest was the Prelog-Djerassi lactone [86] and one of the more recent is ionomycin [87] (Figure 3.8).



**Scheme 3.17.** Evans's asymmetric alkylation of oxazolidinone imides [83].

**Table 3.6.** Alkylations of Evans's oxazolidinone imides (Scheme 3.17 [83]). In all cases, the alkylation products were >99% pure after chromatography.

R	%ds	Yield <sup>1</sup>
Bn	>99	92%
methallyl	98	62%
allyl	98	71%
Et	94	36%

<sup>1</sup> Isolated yields after chromatography.

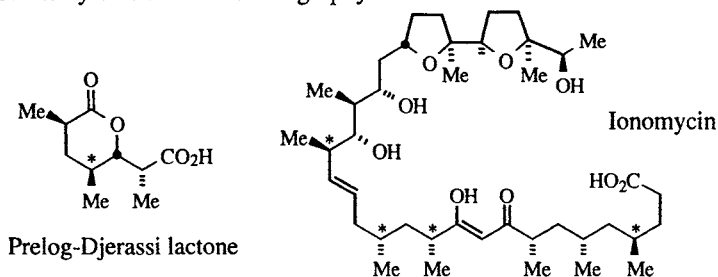
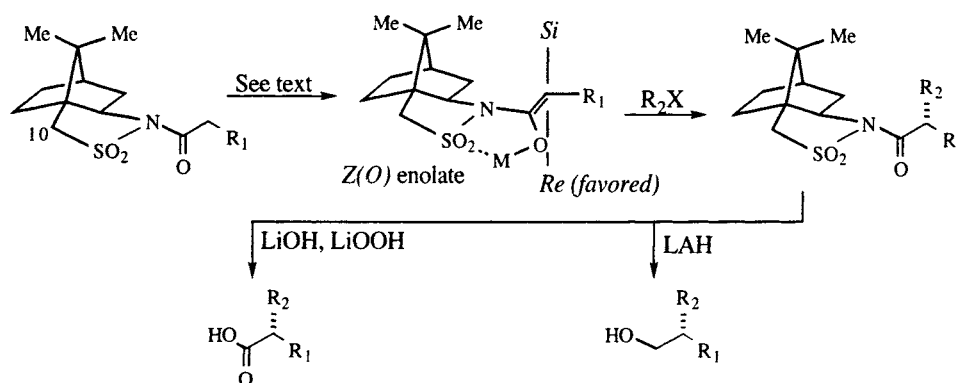


**Figure 3.8.** Syntheses using (in part) asymmetric alkylation of oxazolidinone enolates: Prelog-Djerassi lactone [86] and ionomycin [87]. Stereocenters created by alkylation are indicated (\*).

In addition to these examples of alkylations that employ chelate-enforced intraannular asymmetric induction, Evans's imides are useful in asymmetric aldol (Section 5.2.2 and 5.2.3), and Michael additions (Section 5.3.2), Diels-Alder reactions (Section 6.2.2), and enolate oxidations (Section 8.4), making this one of the most versatile auxiliaries ever invented.

In 1989 Oppolzer reported that the enolates of *N*-acyl sultams derived from camphor afford highly diastereoselective alkylation products with a variety of electrophiles *including those which are not allylically activated* [88]. The sultam is deprotonated using either butyllithium with a catalytic amount of cyclohexyl isopropyl amine, or butyllithium alone, or sodium hexamethyldisilyl amide.<sup>13</sup> As illustrated in Scheme 3.18, alkylation occurs selectively from the *Re* face of the *Z(O)*-enolate to give monoalkylated sultams which can be cleaved by LAH reduction or lithium hydroperoxide catalyzed hydrolysis. Representative examples are listed in Table 3.7.



**Scheme 3.18.** Oppolzer's asymmetric sultam alkylation [88].

**Table 3.7.** Asymmetric alkylation of Oppolzer's sultams (Scheme 3.18) [88].

R <sub>1</sub>	R <sub>2</sub>	%ds	dr <sup>1</sup>	Yield <sup>1</sup>
Me	Bn	98.5	>99:1	89%
Bn	Me	97.4	>99:1	88%
Me	allyl	98.3	>98:2	74%
allyl	Me	97.7	>99:1	2
Me	methallyl	89.6	>99:1	70%
Me	<i>n</i> -C <sub>5</sub> H <sub>11</sub>	98.9	98:2	81%
<i>n</i> -C <sub>5</sub> H <sub>11</sub>	Me	98.1	98:2	2

<sup>1</sup> Diastereomer ratio after recrystallization.

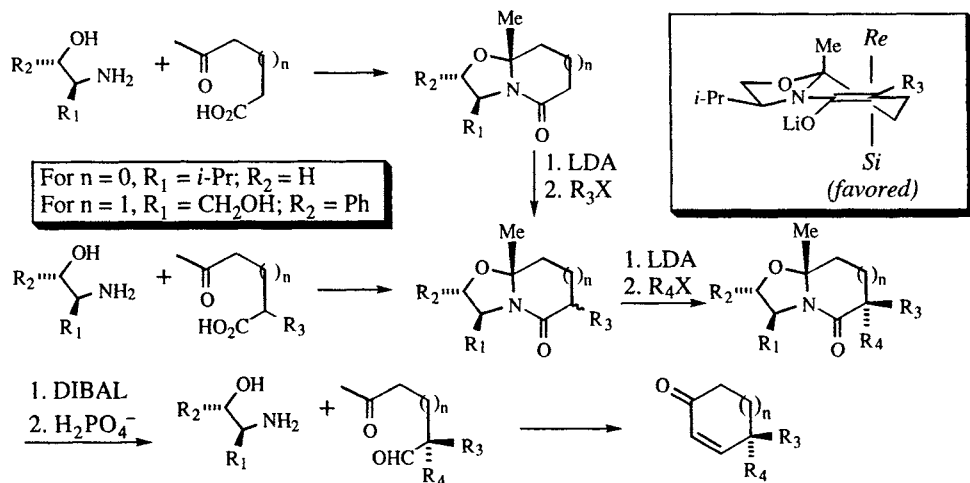
<sup>2</sup> Not reported.

<sup>13</sup> These conditions are necessary to avoid competitive deprotonation at C<sub>10</sub>.

The selectivity of this reaction is based on the following mechanistic rationale of chelate-enforced intraannular asymmetric induction<sup>14</sup> (Scheme 3.18):

1. Following the Ireland model (Scheme 3.4), deprotonation gives the *Z*(*O*)-enolate.
2. The lithium of the enolate is chelated to the sultam which also has a pyramidal nitrogen.
3. The *Si* face is shielded by the bridging methyls, and approach is therefore from the *Re* face, opposite the nitrogen lone pair.

A versatile method for the synthesis of compounds containing quaternary centers (using an intraannular asymmetric induction strategy) was developed by Meyers and uses the bicyclic lactams illustrated in Scheme 3.19 [90-96]. The bicyclic lactams may be synthesized by condensation of an amino alcohol with a keto acid as illustrated [90,95], or by condensation of an amino alcohol with an anhydride followed by reductive cyclization [91]. Sequential alkylations proceed with differing degrees of stereoselectivity. The first alkylation is not very selective, but the second is highly so, as shown by the examples listed in Table 3.8. Note that a different auxiliary is used for the two ring systems. Specifically, for the 5,5-bicyclic system ( $n=0$ ), an auxiliary derived from valinol is used ( $R_1 = i\text{-Pr}$ ,  $R_2 = \text{H}$ ). For the 5,6-bicyclic system, an auxiliary containing a free hydroxyl group is required in order to enable reduction of the carbonyl by intramolecular delivery of hydride at a later stage [93]. In all of the cases reported to date, the two diastereomeric dialkylated bicyclic lactams have been separable by chromatography, insuring enantiomerically pure products at the end. Scheme 3.19 details one protocol for the elaboration of these bicyclic lactams into cyclohexenones, and Scheme 3.20 summarizes different ways that have been developed for the elaboration of the alkylated bicyclic lactams into enantiomerically pure cyclopentenones and cyclohexenones containing chiral quaternary centers of differing substitution patterns [94] (see also ref. [97,98]).



**Scheme 3.19.** Meyers's asymmetric alkylations of bicyclic lactams [90-96]. When  $n = 0$ ,  $R_1 = i\text{-Pr}$  and  $R_2 = \text{H}$ ; when  $n = 1$ ,  $R_1 = \text{CH}_2\text{OH}$  and  $R_2 = \text{Ph}$ .

<sup>14</sup> An alternative explanation, based on analogy of the sultam to a *trans*-2,5-disubstituted pyrrolidine, has also been offered [89].

**Table 3.8** Selected examples of asymmetric alkylation of Meyers's bicyclic lactams

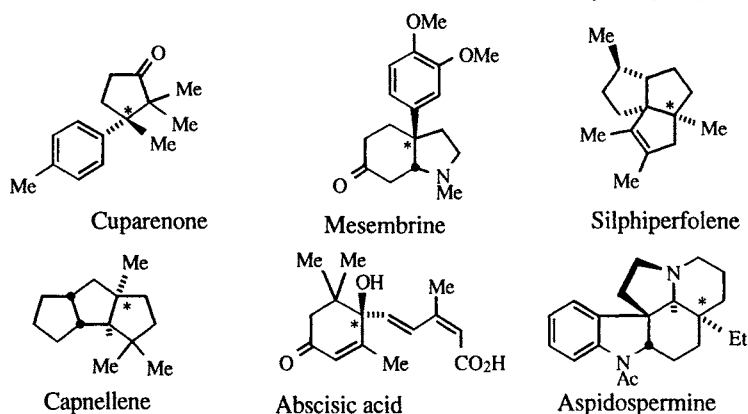


**Figure 3.9.** Natural products synthesized using Meyers's bicyclic lactam methodology: cuparenone [100], mesembrine [101], absciscic acid [102], capnellene [102], silphiperfolene [94], and aspidospermine [103].

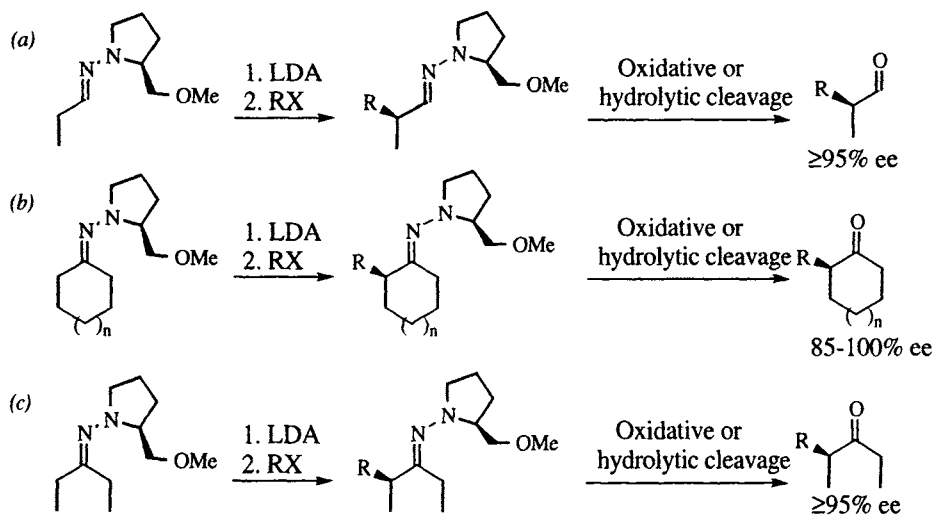
For the asymmetric alkylation of ketones and aldehydes, a highly practical method was developed by the Enders group, and uses SAMP-RAMP hydrazones (reviews: [104-107]). SAMP and RAMP are acronyms for S- or R-1-amino-2-methoxymethylpyrrolidine. This chiral hydrazine is used in an asymmetric version of the dimethylhydrazone methodology originally developed by Corey and Enders [108,109]. These auxiliaries are available from either proline or pyroglutamic acid [104,110]. As shown in Scheme 3.21, SAMP hydrazones of aldehydes [111] and ketones [111,112] may be deprotonated by LDA and alkylated. The diastereoselectivity of the reaction may often be determined by integration of the methoxy singlet after treatment with a shift reagent.<sup>15</sup> After alkylation, cleavage may be effected with a number of reagents [105,106]. Among these are oxidative cleavage by ozonolysis [105], sodium perborate [113], or magnesium peroxyphthalate [114], acidic hydrolysis using methyl iodide and dilute HCl [111,112], or BF<sub>3</sub> and water [115,116]. Table 3.9 lists a few examples of SAMP asymmetric alkylations.

Scheme 3.22 illustrates the mechanistic rationale for this asymmetric alkylation. Deprotonation by the Ireland model (*cf.* Scheme 3.2) gives the *E*<sub>CC</sub>,*Z*<sub>CN</sub> enolate as shown [117].<sup>16</sup> Cryoscopic and spectroscopic measurements indicate that the lithiated hydrazones are monomeric in THF solution [118], and a crystal structure shows the lithium  $\sigma$ -bonded to the azomethine nitrogen and chelated by the methoxy of the auxiliary [119]. The azomethine nitrogen is largely sp<sup>2</sup>-hybridized, and the nitrogen is pulled 'downward' 17.5° below the azaallyl plane by the chelating methoxyl. If this structural feature is preserved in the transition state, the approach of the electrophile toward the *Si* face would be hindered by the C-5 methylene of the pyrrolidine ring and approach toward the *Re* face would be favored, as is observed [119].<sup>17,18</sup> Note that this substructure is equally accessible from both

<sup>15</sup> See Section 2.3.3 for a discussion of the use of lanthanide shift reagents.

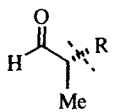
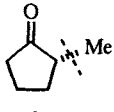
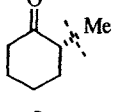
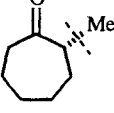
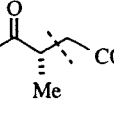
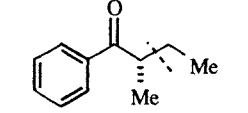
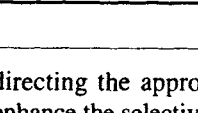
<sup>16</sup> The deprotonation of hydrazones is not regioselective, so the *Z*<sub>CN</sub> geometry results from equilibration *after* deprotonation.

<sup>17</sup> The Agami trajectory (Figure 3.5) would seem to suggest an approach trajectory that is slanted away from the pyrrolidine (*i.e.*, towards the viewer), decreasing the effect of the auxiliary in



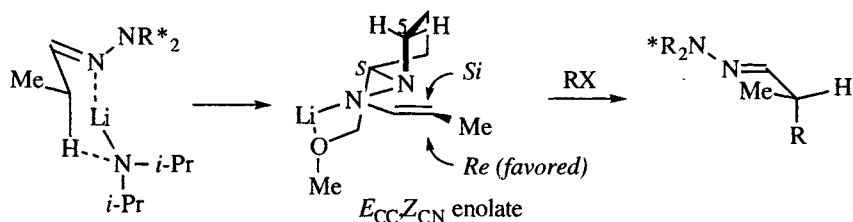
**Scheme 3.21.** Asymmetric alkylations of aldehydes and ketones with SAMP hydrazones.

**Table 3.9.** Asymmetric alkylations of SAMP-RAMP hydrazones (Scheme 3.21 [105]).

Product	Electrophile	% Yield	% ee	Reference
	EtI	71	95	[104,111]
	C <sub>6</sub> H <sub>13</sub> I	52	≥95	
	Me <sub>2</sub> SO <sub>4</sub>	66	86	[111]
	Me <sub>2</sub> SO <sub>4</sub>	70	>99	[111]
	MeI	59	94	[111]
	BrCH <sub>2</sub> CO <sub>2</sub> <i>t</i> -Bu	53	>95	[104]
	EtI	44	>97	[112]

directing the approach. On the other hand, *gem*-dimethyls at the 5-position of the auxiliary enhance the selectivity [119].

<sup>18</sup> Another rationale, which postulates a chelated lithium that is situated on top of the  $\pi$ -cloud of the azaallyl anion, has also been proposed [9,106].



**Scheme 3.22.** Mechanistic rationale for face-selectivity of SAMP hydrazone alkylation [119].

cyclic and acyclic ketones as well as aldehydes. Approach from the *Re* face gives the configuration shown, which is uniformly predictable independent of the ketone or aldehyde educt.

Figure 3.10 illustrates several natural products which have been synthesized using this methodology. These include a number of insect pheromones as well as the sesquiterpene eremophilenolide and the antibiotic X-14547A. The latter two compounds have multiple stereocenters but the asymmetric alkylation using the SAMP-RAMP hydrazone method produces one stereocenter which is then used to direct the selective formation of the others.

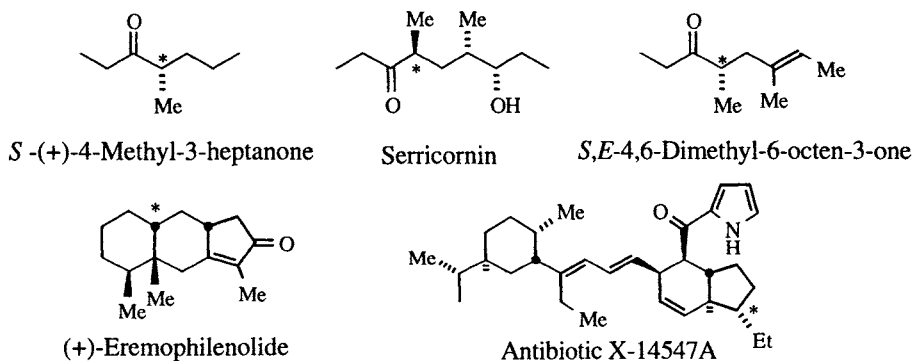


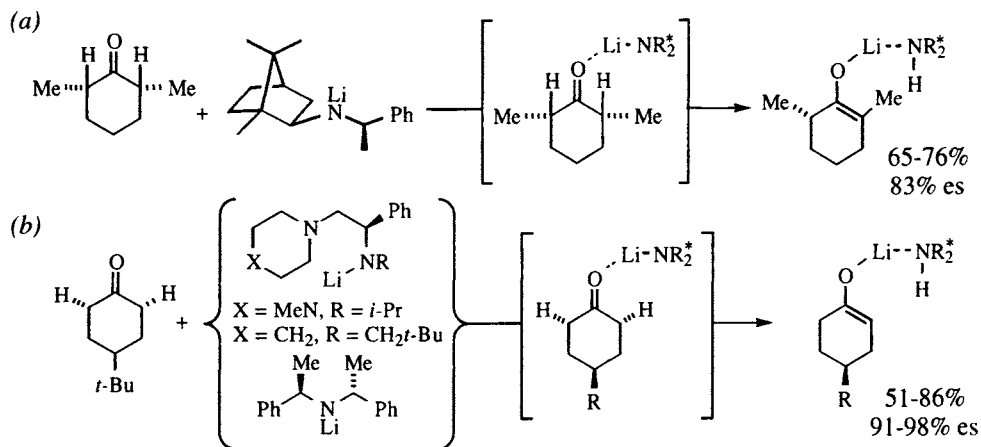
**Figure 3.10** Natural product synthesis employing SAMP-RAMP hydrazones: *S*-(+)-4-methyl-3-heptanone, the leaf cutting ant alarm pheromone [105]; serricornin, the sex pheromone of the cigarette beetle [120]; *S,E*-4,6-dimethyl-6-octen-3-one, the defense substance of “daddy longlegs” [120]; (+)-eremophilenolide [120] and antibiotic X-14547A [121]. Stereocenters formed by asymmetric alkylation are indicated by \*.

*Interligand asymmetric induction.* Group-selective reactions are ones in which



be further manipulated by a number of means. Although crystallographic and spectroscopic characterization of chiral lithium amides have been carried out [125], a rationale explaining the relative topicity of these deprotonations has not been offered. Note that any heterotopic protons may – in principle – be distinguished by this concept. An early contribution to this area was the group-selective deprotonation of cyclohexene oxide, reported by the Whitesell group in 1980 [129], but the selectivities were not high, probably because of minimal prior complexation of the lithium base with the carbon acid.

This concept has been extended to the kinetic resolution (selective reaction of protons that are enantiotopic by external comparison) [30,130] and to selective reaction at proton pairs that are diastereotopic (double asymmetric induction) [131].

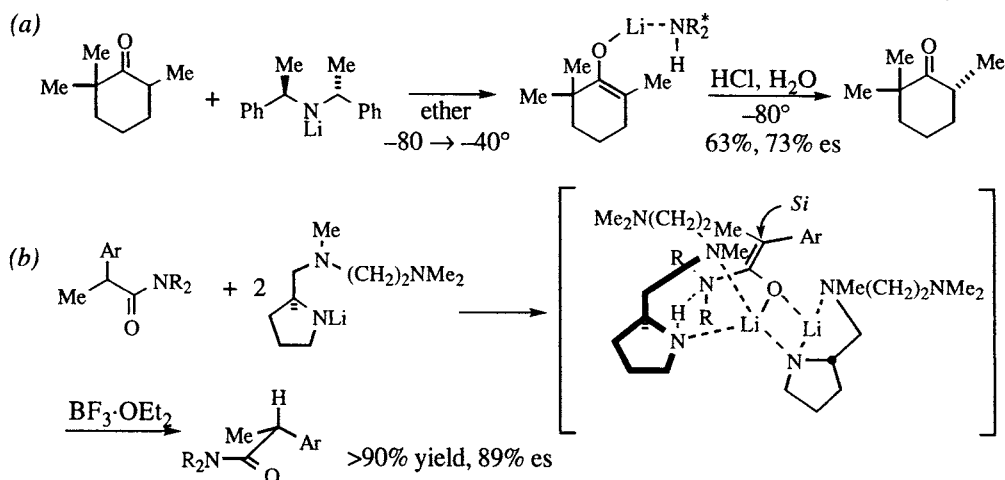


**Scheme 3.23.** Enantioselective deprotonation of achiral ketones with chiral lithium amide bases: (a) [123]. (b) [124-126,128].

A related concept is the selective protonation of enantiotopic faces of an enolate, which is possible because of a combination of two factors:

1. When an enolate-secondary amine complex is quenched with water, the enolate is protonated by internal return from the amine (Scheme 3.2).
2. Complexation with a chiral amine renders the enolate faces diastereotopic.

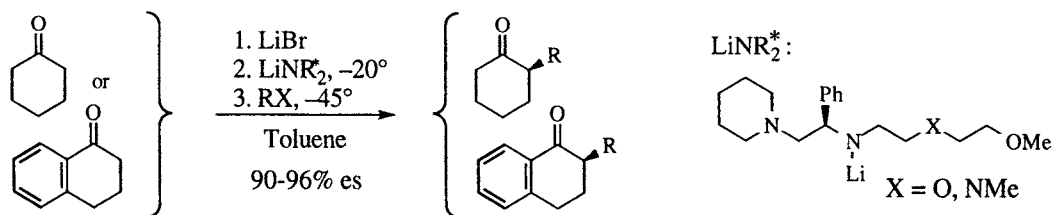
Thus, use of a chiral lithium amide base followed by protonation by internal return may be enantioselective because of interligand asymmetric induction. Scheme 3.24a shows an example reported in 1982 by Hogeveen [30,122]. In competition with protonation of the enolate by proton transfer from the amine is direct protonation by water, which has the effect of lowering the enantioselectivity of the process. A recent contribution by Vedejs [32,132] notes that the intermolecular route can be avoided by quenching the enolate-amine complex with an aprotic acid such as boron trifluoride, and excellent selectivities were obtained in certain instances (e.g., Scheme 3.24b). The aggregate proposed to account for these selectivities is illustrated in Scheme 3.24b. The argument is that the amide nitrogen ( $\text{NR}_2$ ) is rotated out of plane and is hydrogen bonded to the amine  $\text{NH}$ . Complexation of the amine nitrogen by boron increases the acidity of the  $\text{N-H}$  ('ammonium-like'), and the proton is then transferred to the nearest ( $\text{Si}$ ) face of the enolate. At this point in time, no method offers a *substrate-independent* asymmetric



**Scheme 3.24.** Intramolecular enantioselective protonation of an enolate. The lithium amides are illustrated as monomers for simplicity; the aggregation states are unknown. (a) [30,122]. (b) [32,132].

protonation protocol, but progress is being made (review: [133]; see also ref. [24,32,134-140]).

A further extension of these concepts is the alkylation of enolate / secondary amine complexes. Following several early observations [141-143],<sup>19</sup> systematic investigations were undertaken by the Koga group [24,25,147-149]. These efforts have resulted in a very selective asymmetric alkylation of cyclohexanone and  $\alpha$ -tetralone with activated alkyl halides (Scheme 3.25). As listed in Table 3.10, alkylation of these ketones affords up to 96% enantioselectivity. During the optimization studies, Koga observed an increase in enantioselectivity and chemical yield as the reaction time increased, and ascribed the phenomenon to the formation of a mixed aggregate that includes the lithium bromide formed as the reaction proceeds. Further experiments revealed that addition of one equivalent of lithium



**Scheme 3.25.** Enantioselective alkylation of lithium enolate/secondary amine/lithium bromide complexes by interligand asymmetric induction [148,149].

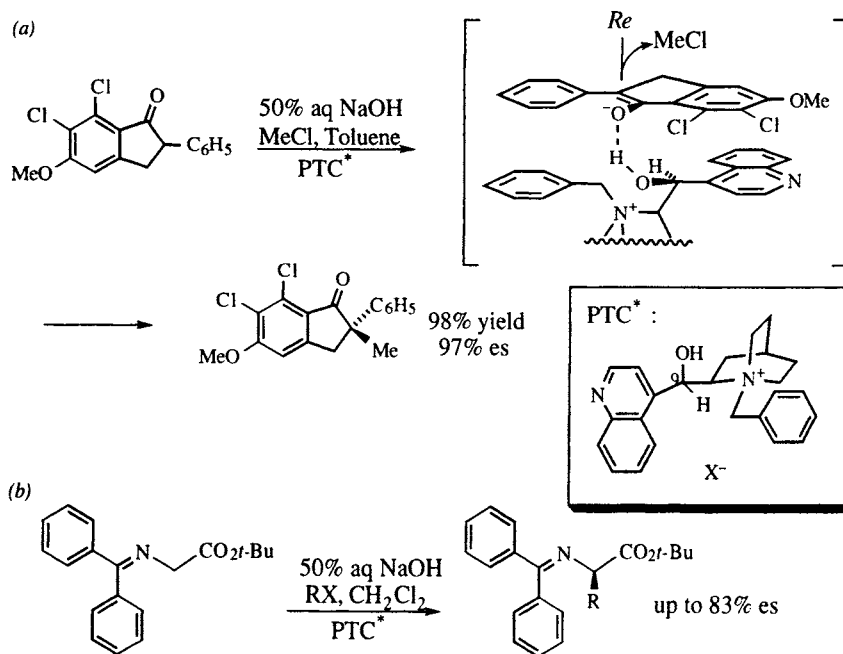
<sup>19</sup> It has even been noted that deprotonation of some chiral, nonracemic carbonyl compounds by an achiral base affords an enolate that is chiral (having a chirality axis or a chelating atom that becomes stereogenic upon coordination to the lithium, for example) and nonracemic, and which affords nonracemic products upon alkylation [144-146], but a mechanistic rationale has not been established.

**Table 3.10.** Koga's asymmetric alkylation of ketones (Scheme 3.25 [148])

Ketone	Electrophile	Yield	% es
cyclohexanone	PhCH <sub>2</sub> Br	63%	96
cyclohexanone	PhCH=CHCH <sub>2</sub> Br	60%	94
cyclohexanone	CH <sub>2</sub> =CHCH <sub>2</sub> Br	41%	90
$\alpha$ -tetralone	PhCH <sub>2</sub> Br	89%	96
$\alpha$ -tetralone	PhCH=CHCH <sub>2</sub> Br	93%	94
$\alpha$ -tetralone	MeI	71%	94

bromide at the beginning of the reaction optimizes the stereoselectivity. The reactive species is thought to be a lithium enolate / secondary amine / lithium bromide mixed aggregate [148]. A rationale for the stereoselectivity of this process has yet to emerge, and the generality of it is limited. It does, however, foretell of more general successes to come.

A conceptually different approach to interligand asymmetric induction uses chiral phase transfer catalysts. Scheme 3.26 illustrates two examples of such a process using an *N*-benzylcinchonium halide catalyst. The first is an indanone methylation [150] and the second is a glycine alkylation [151]. Hughes *et al.* reported a detailed kinetic study of the indanone methylation which revealed a mechanism significantly more complicated than a simple phase-transfer process: the reaction is 0.55 order in catalyst and 0.7 order in methyl chloride, deprotonation of the indanone occurs at the interface, and methylation of the enolate (not deprotonation) is rate-determining [150]. Nevertheless, the rationale for the

**Scheme 3.26.** Enantioselective alkylations using chiral phase-transfer catalysts. (a) [150], (b) [151].

enantioselectivity involves a 1:1 complex of catalyst and enolate, as illustrated in Scheme 3.26a. Molecular modeling studies and an X-ray crystal structure suggest that the most stable conformation of the catalyst has the quinoline ring, the C<sub>9</sub>–O bond, and the *N*-benzyl group nearly coplanar [150]. Hydrogen bonding with the enolate, dipole alignment, and  $\pi$ -stacking of the aromatic moieties result in the assembly shown. Methylation then occurs from the *Re* face, opposite the catalyst.

O'Donnell reported the asymmetric alkylation of the Schiff base of *tert*-butyl glycinate using *N*-benzylcinchonium chloride (Scheme 3.26b, [151]). This process, which works for methyl, primary alkyl, allyl, and benzyl halides (Table 3.11), is noteworthy because the substrate is acyclic and because monoalkylation is achieved without racemization under the reaction conditions. The observed chirality sense may be rationalized by assuming an *E(O)*-enolate and  $\pi$ -stacking of the benzophenone rings of the enolate above the quinoline ring on the catalyst, and approach of the electrophile as before.

**Table 3.11.** O'Donnell's asymmetric glycine alkylations by chiral phase transfer catalysis (Scheme 3.26b [151]).

RX	Yield	% es
MeBr	60%	71
<i>n</i> -BuBr	61%	76
CH <sub>2</sub> =CHCH <sub>2</sub> Br	75%	83
PhCH <sub>2</sub> Br	75%	83

The lack of racemization and dialkylation in this process deserves comment. Apparently, the rate of deprotonation of the product is significantly slower than deprotonation of the starting material. The reasons for the reduced acidity of the product become apparent upon examination of models (Figure 3.11).<sup>20</sup> A<sup>1,3</sup> strain considerations dictate that the  $\alpha$ -carbon-hydrogen bond (nearly) eclipses the nitrogen-carbon double bond and also forces the syn phenyl group out of planarity. The three lowest energy conformers<sup>21</sup> are illustrated looking down the  $\alpha$ -carbon–nitrogen bond. The global minimum (conformation *a*) has the  $\alpha$ -proton near the nodal plane of the carbonyl  $\pi$ -system, and therefore nonacidic. The other two have the  $\alpha$ -proton in better alignment with the carbonyl, but shielded from the approach of the base by the phenyl group at the top. Note that a proton in the position of the  $\alpha$ -methyl in conformation *a* (as in the starting material) would be quite acidic due to overlap with *both*  $\pi$ -systems. Additionally, to the extent that the proximal phenyl

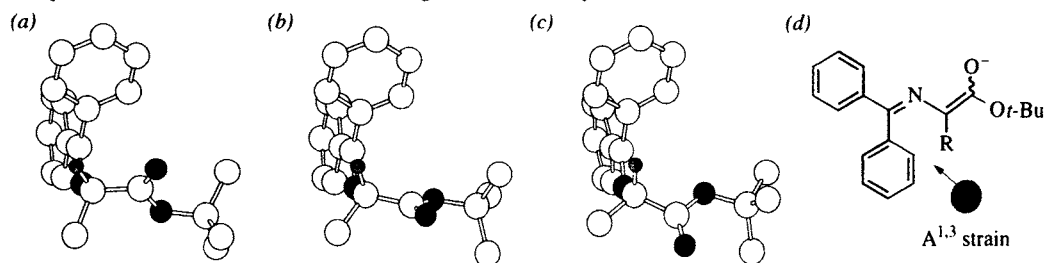


**Figure 3.11.** (a)-(c) Low energy conformations of *tert*-butyl alaninate-benzophenone Schiff base. Only the  $\alpha$ -hydrogen is shown (hydrogen is shaded, nitrogen and oxygen are black).  $E_{rel}$  (kcal/mole): a, 0; b, +0.10; c, +0.14. (d) Substituted enolate, showing allylic strain due to the R group.

## 3.2 Chiral organolithiums

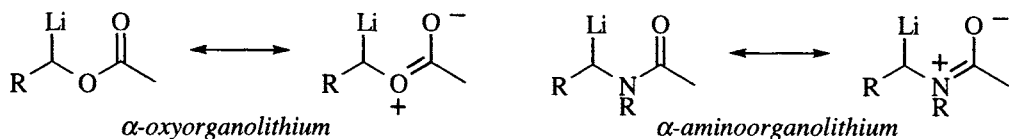
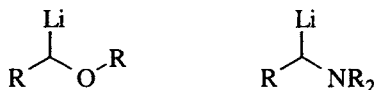
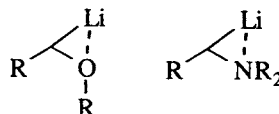
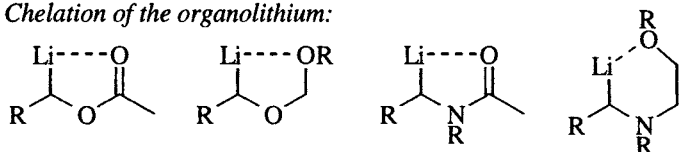
*sec*-Butyllithium is chiral, but it is usually found in racemic form.<sup>22</sup> Indeed, many secondary organolithiums (and Grignard reagents) are chiral, but those used in asymmetric synthesis have been mostly limited to  $\alpha$ -heteroatom organometallics.<sup>23</sup> In contrast to resonance stabilized anions,  $\alpha$ -heteroatom 'carbanions' are stabilized by inductive and dipole effects, or both, and sometimes by chelation [156]. The heteroatom may be a first row element such as nitrogen or oxygen, or main group elements such as phosphorous, sulfur, selenium, or tellurium. In most of these cases, the carbon bearing the metal is tetrahedral, and may be stereogenic. The following sections focus on organolithium species, where the heteroatom is either an oxygen or a nitrogen. Two types of species are discussed, those in which the negative charge on carbon is stabilized by a dipole, so-called dipole-stabilized anions, and those in which the inductive electron withdrawal of the heteroatom is the major contributor (Figure 3.12). There is ample evidence, both theoretical [157-159] and structural [160,161], that dipole-stabilized organometallics are chelated by the carbonyl oxygen. There is also good evidence that inductively stabilized  $\alpha$ -heteroatom organolithiums have the metal bridged across the carbon-heteroatom bond [161,162]. Note that a distinction is made between bridging and chelation, even though the former might be called  $\alpha$ -chelation. The simple reason is that there are distinct differences in stability and reactivity between the two types of compounds (*e.g.*, see ref. [163]).

When contemplating the use of stereogenic 'carbanions' in the synthesis of non-racemic compounds, one must consider several factors (Scheme 3.27):

1. Is the organolithium configurationally stable (Scheme 3.27a)?
2. Does the reaction with an electrophile proceed with retention or inversion of configuration at the carbanionic carbon (Scheme 3.27b)?

<sup>22</sup> Reich has shown that 2° alkylolithiums possess reasonable configurational stability, even in THF [153].

<sup>23</sup> An interesting recent development employs an asymmetric transformation to enantioselectively alkylate benzylic organolithiums in the presence of sparteine [154,155].

*Dipole-stabilized organolithiums:**Organolithiums stabilized by inductive effects:**Lithium bridging:**Chelation of the organolithium:*

**Figure 3.12.** Classification of  $\alpha$ -oxy- and  $\alpha$ -aminoorganolithiums as either dipole-stabilized or inductively stabilized. Metal atom bridging and internal chelation may also play a role in both stabilization and chemical properties such as configurational stability.

3. If the electrophile is an aldehyde or an unsymmetrical ketone, does the organometallic add selectively to one of the heterotopic faces (Scheme 3.27c)?
4. What is the aggregation state of the organometallic? If there are aggregates, are they homochiral or heterochiral? If there is more than one species present in solution, which one is responsible for the observed behavior (Scheme 3.27d)?

Answering these questions is not always possible; but without answers, mechanistic interpretation is speculative, at best.

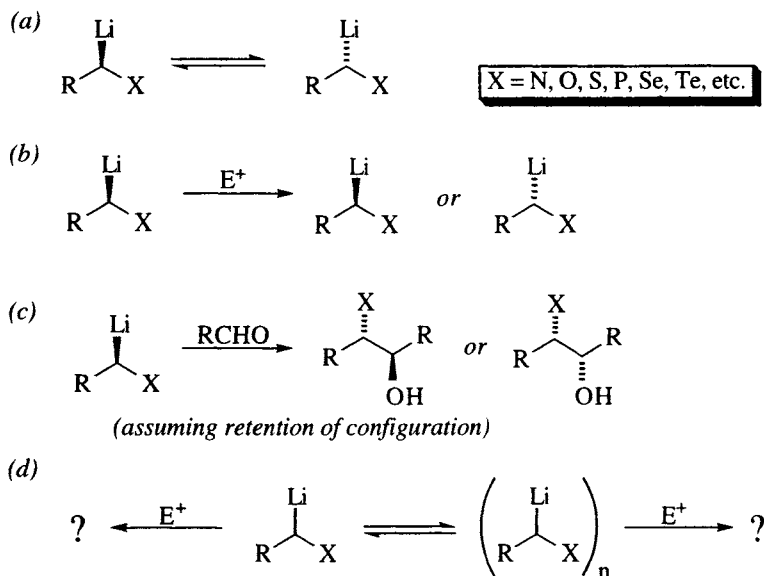
### 3.2.1 $\alpha$ -Alkoxyorganolithiums<sup>24</sup>

$\alpha$ -Alkoxy carbanions can be obtained by deprotonation or by exchange with another atom, most commonly with tin. In 1980, Still reported that the  $\alpha$ -alkoxyorganolithium reagents derived from tin-lithium exchange of  $\alpha$ -alkoxyorganostannanes are configurationally stable [165].<sup>25</sup> The tin-lithium exchange reaction takes place with retention of configuration [165,167],<sup>26</sup> so obtaining an  $\alpha$ -alkoxyorganolithium of known configuration is predicated on having an  $\alpha$ -alkoxyorganostannane of known configuration. These are made by *O*-alkylation of the corresponding  $\alpha$ -hydroxystannanes, which are in turn formed by asymmetric reduction (Chapter 7) of an acyl stannane [169-171], kinetic resolution using a lipase enzyme [172], or oxidation of  $\alpha$ -stannylboronates [173]. Enantiomeric purities of the  $\alpha$ -alkoxystannanes thus obtained are often in the 95% range.

<sup>24</sup> For a review of  $\alpha$ -alkoxyorganolithiums in coupling reactions, see ref. [164].

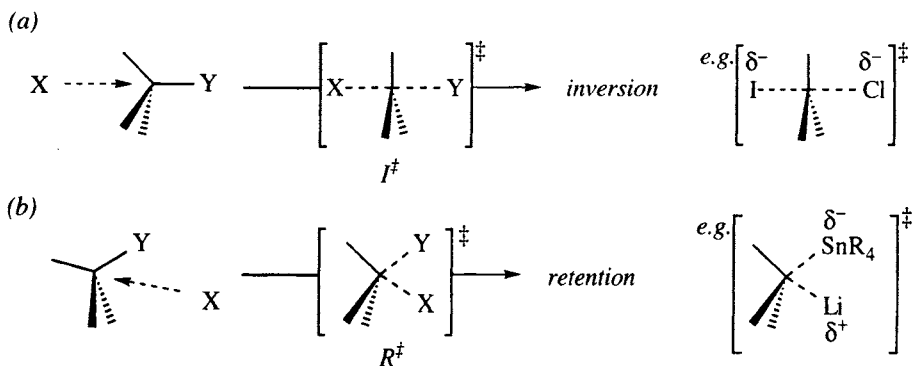
<sup>25</sup> For a theoretical explanation of this stability, see ref. [166].

<sup>26</sup> The stereochemical course at tin depends on the tin ligands and the solvent [168].



**Scheme 3.27.** Factors to consider in evaluating reactions of chiral organolithiums.

The reason tin-lithium exchange proceeds with retention may be understood by consideration of the two transition structures ( $I^\ddagger$  and  $R^\ddagger$ ) for bimolecular substitution shown in Scheme 3.28. The  $S_N2$  reaction occurs with inversion of configuration. Note that in the  $I^\ddagger$  transition structure for the reaction  $I^- + RCl$  (Scheme 3.28a), the nucleophile and the leaving group both carry partial negative charges, which are better accommodated by  $I^\ddagger$  than by  $R^\ddagger$ , simply because of Coulombic repulsion. In the tin-lithium exchange ( $S_E2$  reaction), the lithium replaces the pentavalent tin of an ate-complex, so that in the transition state, the lithium carries a partial positive charge, while there is still a partial negative charge on tin. Coulombic attraction suggests that  $R^\ddagger$  should be favored in this case (Scheme 3.28b).<sup>27</sup>



**Scheme 3.28.** (a) Bimolecular inversion reaction and transition state, typified by  $S_N2$  reaction. (b) Bimolecular reaction with retention, typified by tin-lithium exchange.

<sup>27</sup> In some electrophilic substitutions, reagent X initially coordinates to Y and the  $R^\ddagger$  transition state is cyclic. For a thorough account of the many types of electrophilic substitutions, see ref. [174].

Deprotonation of ethers is another route to the  $\alpha$ -alkoxy anions, but this pathway is often precluded by a kinetic barrier. Unless the  $\alpha$ -carbon is benzylic [175], surmounting this barrier usually requires conditions that are not favorable to the survival of the anion [164]. Notable exceptions are the hindered aryl esters studied by Beak [176], Figure 3.13a, and the carbamates studied by Hoppe [177], shown in Figure 3.13b. In both cases, *sec*-butyllithium is required for deprotonation, and the carbonyls which direct the metalation by a complex-induced proximity effect [178] must be shielded from the base by large alkyl groups. Once formed, the organolithiums are chelated and stabilized by the heteroatom-induced dipole [179].

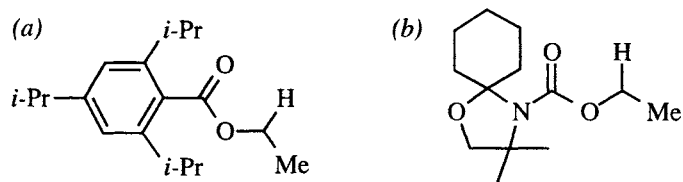


**Figure 3.13.** Substrates that may be deprotonated by butyllithium bases  $\alpha$  to nitrogen. In both cases the bulk of the carbonyl moiety opposite the ethoxy group shields the carbonyl from nucleophilic attack. (a) Trisopropyl benzoates [176]. (b) Oxazolidine carbamates [177].

Reaction with carbonyl electrophiles is possible, so enantiopure stannanes are excellent precursors of enantiopure  $\alpha$ -alkoxy tertiary alcohols [165,167],  $\alpha$ -alkoxy acids and esters [180], and  $\alpha$ -alkoxyketones [181], and  $\gamma$ -alkoxyhydrazides (precursor-

**Table 3.12.** Stereospecific reactions of  $\alpha$ -alkoxyorganolithiums with electrophiles.

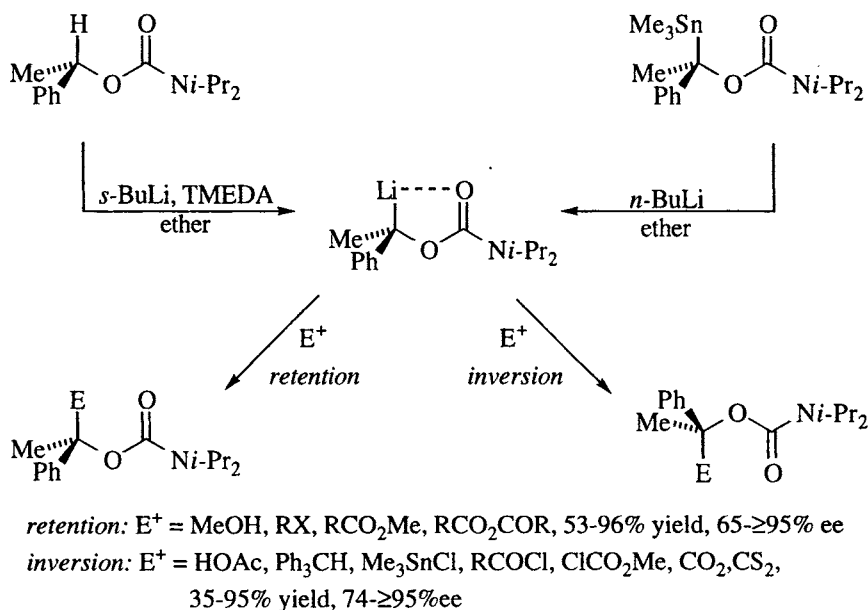
Entry	Stannane	Electrophile	Product	% Yield	Ref.
1		acetone		90	[165]
2		CO <sub>2</sub>		93	[180]
3		ClCO <sub>2</sub> Me		71	[180]
4		RCONMe <sub>2</sub>		76	[181]
5		CH <sub>2</sub> =CHCON <sub>2</sub> Me <sub>3</sub>		50	[182]



sors to  $\gamma$ -lactones) [182], as the examples in Table 3.12 illustrate. Note however, that addition of these nucleophiles to aldehydes and unsymmetric ketones is not diastereoselective. Unfortunately, the reaction of these  $\alpha$ -alkoxyorganolithiums with alkyl halides is usually inefficient and not stereoselective due to the intervention of single electron transfer processes [167]. Methylation can be achieved with dimethyl sulfate, however [165,167], and silylation is stereospecific [165].

The carbamates in Figure 3.13b deserve special mention because Hoppe has shown that a complex of *sec*-butyllithium and sparteine (an inexpensive, chiral, tetramelic diamine) demonstrates  $O$ -ethyl,  $O$ -butyl,  $O$ -isobutyl, and  $O$ -hexyl (i.e.,

It may be tempting to assume that similar organolithiums would also alkylate with retention of configuration at the metal-bearing carbon. Not so. Unlike  $S_N2$  reactions, transition states for  $S_E2$  electrophilic substitution reactions giving retention ( $R^\ddagger$ , Scheme 3.28) and inversion ( $I^\ddagger$ ) are not far apart in energy [186], and both reaction manifolds are common. For example, the carbamate shown in Scheme 3.30 affords products of either retention or inversion, depending on the electrophile: esters, anhydrides, and alkyl halides afford products of retention whereas acid chlorides, acyl cyanides, carbon dioxide, carbon disulfide, isocyanates, and tin chlorides afford products of inversion [184,187]. Interestingly, this *acyloxyorganolithium* reacts well with alkyl halides, unlike the *alkoxyorganolithiums* listed in Table 3.12.



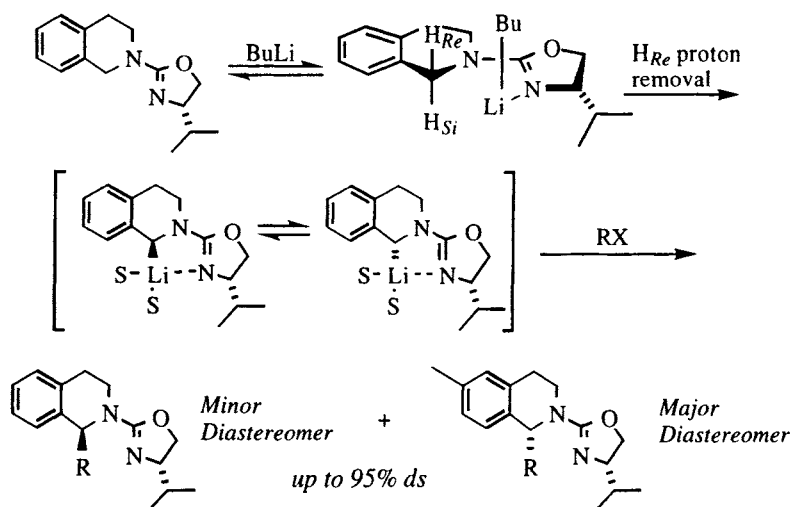
**Scheme 3.30.** The stereochemical course of the alkylation of chiral organolithiums may depend on the electrophile [184,187].

The authors speculate that the stereochemical divergence may be related to the ability of the electrophile to coordinate with the lithium, coupled with the presence or absence of a low-lying LUMO. Curiously, protonation by methanol proceeds with retention whereas protonation with either acetic acid or triphenyl methane proceeds with inversion. The authors speculate that, in acetic acid, protonation of the TMEDA nitrogen and internal return (*cf.* Schemes 3.2 and 3.24) may occur instead of direct protonation [184]. Presumably, direct protonation is the only mechanistic course with weak acids such as methanol and triphenylmethane and steric effects dictate inversion for the latter. Hoppe also noted that the enantiomeric purity of the products also depended on the solvent. In THF, the products were nearly racemic, and the enantiomeric purity of several of the other alkylation products was variable in solvents such as ether and pentane. This variability is due, at least in part, to the degree of covalency of the C–Li bond. In donor solvents such as THF, racemization is more facile.

3.2.2  $\alpha$ -Aminoorganolithiums<sup>28</sup>

Because nitrogen is trivalent, it is possible to attach a third substituent, often an activating group or a chiral auxiliary that facilitates either deprotonation or stereoselective alkylation, or both. Most commonly, dipole-stabilized [179,189]  $\alpha$ -aminoorganolithiums have been used. As with the  $\alpha$ -oxyorganolithiums discussed in the previous section,  $\alpha$ -lithiated amines feature pyramidal carbanionic carbons, and can be formed either by deprotonation or by tin-lithium exchange, although deprotonation of an unactivated (nonallylic or nonbenzylic) position has a fairly high kinetic barrier.

The barrier to pyramidal inversion of acyclic dipole-stabilized  $\alpha$ -aminoorganolithiums is considerably lower than the inversion barrier for  $\alpha$ -alkoxyorganolithiums, so temperatures near  $-100^\circ\text{C}$  are necessary to maintain configurational integrity [190,191]. For allylic or benzylic dipole-stabilized  $\alpha$ -aminoorganolithiums, it appears that pyramidal inversion cannot be prevented even at such low temperature [192,193]. Recall that an enantioselective deprotonation was the source of the enantioselectivity in the alkylation of dipole-stabilized  $\alpha$ -oxyorganolithiums (Scheme 3.29), and that benzylic dipole-stabilized  $\alpha$ -oxyorganolithiums were found to be configurationally stable (Scheme 3.30). Detailed mechanistic studies of the lithiation of tetrahydroisoquinolines having formamidine or oxazoline chiral auxiliaries have shown that the deprotonation is stereoselective [192,194], but in the oxazolines (Scheme 3.31,  $H_{Re}$  removal favored *via* the postulated coordination complex shown), the selectivity of the bond-forming step is determined later [192]. Specifically, stereoselective deuteration at C-1 and analysis of the alkylation products for both deuterium content and diastereomer ratio showed that – even when the stereoselectivity of the deprotonation is reduced to zero by an isotope effect – the diastereomer ratio in the product is unchanged. There are two limiting



**Scheme 3.31.** Mechanism for asymmetric alkylation of a tetrahydroisoquinoline using an oxazoline auxiliary [192].

<sup>28</sup> For a review of alkylations of nitrogen-stabilized carbanions, see ref. [188].

possibilities for the source of the observed selectivity: an unbalanced equilibrium of organolithium diastereomers and a fast alkylation compared to inversion (thermodynamic effect), or a fast equilibrium coupled to energetically nonequivalent transition states (Curtin-Hammett kinetics [195,196]). Because of uncertainties in the position of the organolithium equilibrium, the reaction state of the

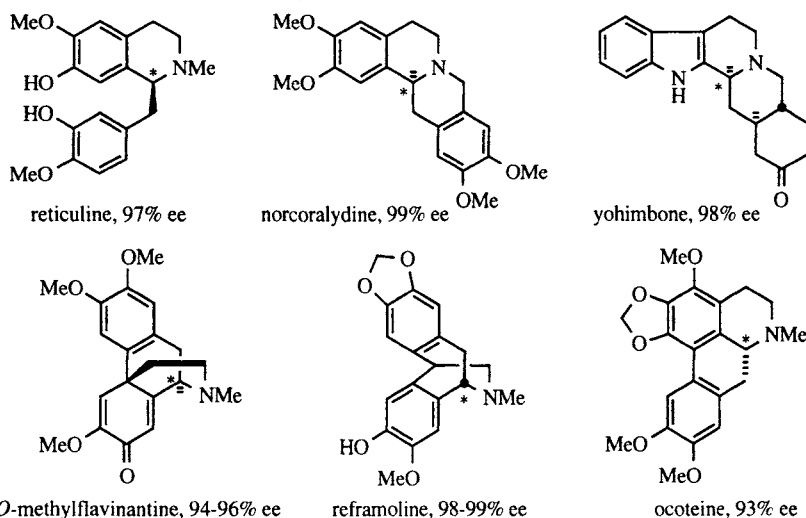
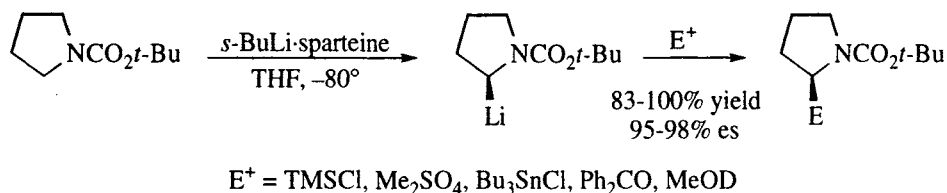


**Figure 3.14.** Natural products synthesized using the asymmetric alkylation strategy: reticuline [205], norcoralydine [206,207], yohimbone [208], *O*-methylflavinantine [209], reframoline [207], and ocoteine [206,207]. The stereocenter formed by asymmetric alkylation is indicated with \*.

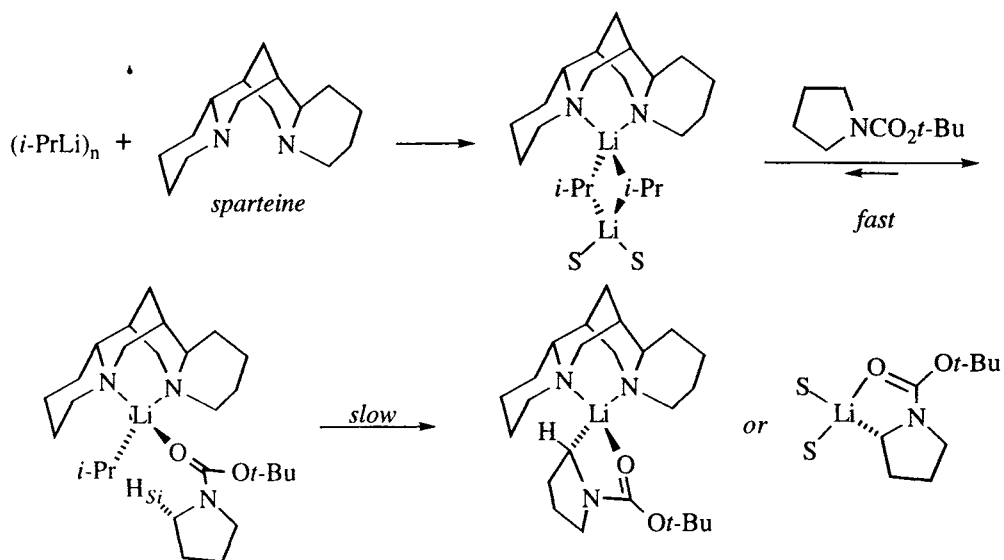
Scheme 3.33 [204,210].<sup>29</sup> A limitation of this method is the failure of the organolithium to react efficiently with alkyl halide electrophiles.

The mechanism of this reaction has been studied by Beak and his group. Pertinent aspects are illustrated in Scheme 3.34. NMR studies indicate that sparteine and isopropyllithium form an unsymmetrical complex wherein one of the lithiums of the isopropyllithium dimer is chelated by sparteine while the other is not [211]. Kinetic studies indicate that when BOC-pyrrolidine is added to this complex, an equilibrium is established with a ternary complex of isopropyllithium, sparteine, and BOC-pyrrolidine (favoring the ternary complex with an equilibrium constant  $\geq 300$ ). Although the structure of this complex is not known, it is difficult to imagine that coordination of the BOC-pyrrolidine to the distal (unchelated) lithium would afford a species that is likely to react enantioselectively, so Beak suggests that the most likely possibility is the complex shown in the lower left of Scheme 3.34 [210,212]. The kinetic data further indicate that the deprotonation step is rate determining [212]. Beak suggests that a conformation such as the one illustrated presents the  $H_{Si}$  proton to the alkylolithium [210].



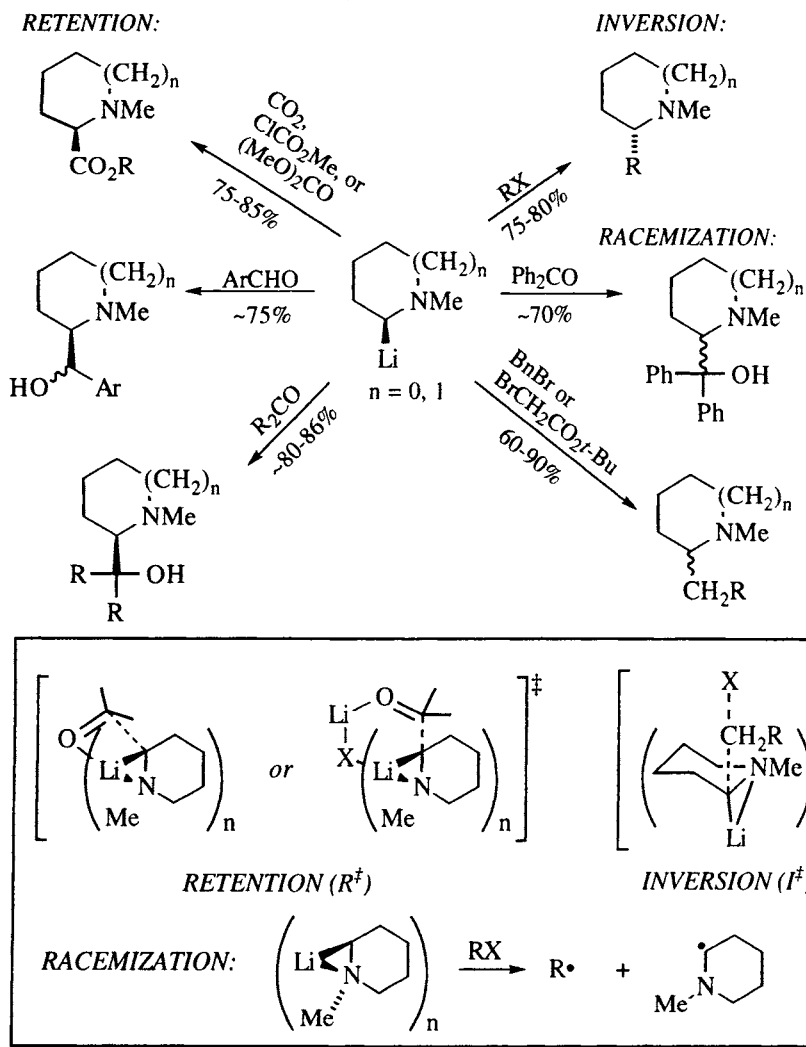
**Scheme 3.33.** Asymmetric deprotonation and electrophilic substitution of BOC-pyrrolidine [204,210].

<sup>29</sup> Attempts to enantioselectively deprotonate BOC-piperidine with *s*-BuLi·sparteine failed [D. Hoppe, private communication].



**Scheme 3.34.** Postulated mechanism for the asymmetric deprotonation of BOC-pyrrolidine [212].

The chemistry of lithiated *N*-methylpiperidines and *N*-methylpyrrolidines,  $\alpha$ -aminoorganolithiums that are not dipole-stabilized, exhibits features that are quite distinct from those found for lithiated dipole-stabilized heterocycles. First of all, 2-lithio-*N*-methylpiperidine and 2-lithio-*N*-methylpyrrolidine possess the greatest configurational stability of any  $\alpha$ -aminoorganolithium known: in the presence of TMEDA, they are configurationally stable at temperatures as high as  $-40^\circ\text{C}$ , and are more prone to chemical decomposition than racemization [163,213]. Second, they react smoothly with alkyl halides (Scheme 3.35) more efficiently than either lithiated formamidines [214] or BOC heterocycles [215,216]. Third, the mechanistic (and stereochemical) course of their electrophilic substitution reactions depend on the electrophile in a unique way [217]. These organolithium compounds are obtained by tin-lithium exchange from the corresponding stannane; examples of their reactivity are shown in Scheme 3.35 [217]. With most carbonyl electrophiles retention of configuration is observed, whereas with alkyl halides, inversion is observed. When the electrophile is easily reduced, as with benzophenone or *tert*-butyl bromoacetate, the products are racemic. It is thought that the reactions affording racemic products proceed by a single electron transfer (radical) mechanism, while the others go by  $R^\ddagger$  or  $I^\ddagger$  (recall Scheme 3.28) mechanisms, as shown in the inset in Scheme 3.35 [217]. Note, however, that the dichotomy observed in these reactions bears no resemblance to the dichotomy observed by Hoppe in  $\alpha$ -oxyorganolithium reactions, which occurred with different carbonyl electrophiles and which was attributed to a low-lying LUMO (Scheme 3.30 [184]). For both types of organolithium compounds, a firm mechanistic basis for this dichotomy has yet to be established. Moreover, comparison of the varied reactivities of dipole-stabilized and inductively stabilized  $\alpha$ -aminoorganolithiums reveal a clear difference in reactivity pattern.



**Scheme 3.35.** 2-Lithio *N*-methylpiperidines and pyrrolidines are versatile reagents in electrophilic substitutions. The stereochemical course of the reaction depends on the electrophile. *Inset*: proposed transition structures for the  $R^\ddagger$  and  $I^\ddagger$  reactions, and SET mechanistic proposal for the electrophiles that afford racemic products [217].

### 3.3 References

1. D. J. Cram *Fundamentals of Carbanion Chemistry*; Academic: New York, 1965.
2. J. C. Stowell *Carbanions in Organic Synthesis*; Wiley: New York, 1979.
3. R. B. Bates *Carbanions*; Springer-Verlag: Berlin, 1983.
4. *Comprehensive Carbanion Chemistry*; E. Buncl; T. Durst, Eds.; Elsevier: Amsterdam, 1980.
5. D. Seebach *Angew. Chem. Int. Ed. Engl.* **1988**, 27, 1624-1654.
6. G. Boche *Angew. Chem. Int. Ed. Engl.* **1989**, 28, 277-297.
7. E. S. Gould *Mechanism and Structure in Organic Chemistry*; Holt, Rinehart and Winston: New York, 1959.

8. D. Caine In *Carbon-Carbon Bond Formation*; R. L. Augustine, Ed.; Marcel Dekker: New York, 1979, p 85-352.
9. D. Caine In *Comprehensive Organic Synthesis. Selectivity, Strategy, and Efficiency in Modern Organic Chemistry*; B. M. Trost, I. Fleming, Eds.; Pergamon: Oxford, 1991; Vol. 3, p 1-63.
10. J.-M. Lehn *Pure Appl. Chem.* **1978**, *50*, 871-892.
11. J.-M. Lehn *Angew. Chem. Int. Ed. Engl.* **1988**, *27*, 89-112.
12. J. d'Angelo *Tetrahedron* **1976**, *32*, 2979-2990.
13. L. M. Jackman; B. C. Lange *Tetrahedron* **1977**, *33*, 2737-2769.
14. D. A. Evans In *Asymmetric Synthesis*; J. D. Morrison, Ed.; Academic: Orlando, 1984; Vol. 3, p 1-110.
15. P. G. W. M. J. Hintze *J. Am. Chem. Soc.* **1990**, *112*, 8602-8604.
16. E. M. Arnett; F. G. Fischer; M. A. Nichols; A. A. Ribiero *J. Am. Chem. Soc.* **1990**, *112*, 801-808.
17. K. Sakuma; J. H. Gilchrist; F. E. Romesberg; C. E. Cajthami; D. B. Collum *Tetrahedron Lett.* **1993**, *34*, 5213-5216.
18. A. J. Edwards; S. Hockey; F. S. Mair; P. R. Raithby; R. Snaith; N. S. Simpkins *J. Org. Chem.* **1993**, *58*, 6942-6943.
19. M. T. Reetz; S. Hütte; R. Goddard *J. Am. Chem. Soc.* **1993**, *115*, 9339-9340.
20. L. M. Jackman; T. S. Dunne *J. Am. Chem. Soc.* **1985**, *107*, 2805-2806.
21. H. Estermann; D. Seebach *Helv. Chim. Acta* **1988**, *71*, 1824-1839.
22. K. Narasaka; Y. Ukaji; K. Watanabe *Chem. Lett.* **1986**, 1755-1758.
23. B. J. Bunn; N. S. Simpkins *J. Org. Chem.* **1993**, *58*, 533-534.
24. T. Yasukata; K. Koga *Tetrahedron Asymmetry* **1993**, *4*, 35-38.
25. Y. Hasegawa; H. Kawasaki; K. Koga *Tetrahedron Lett.* **1993**, *34*, 1963-1966.
26. P. L. Creger *J. Am. Chem. Soc.* **1970**, *92*, 1396-1397.
27. D. Seebach; M. Boes; R. Naef; W. B. Schweizer *J. Am. Chem. Soc.* **1983**, *105*, 5390-5398.
28. J. D. Aebi; D. Seebach *Helv. Chim. Acta* **1985**, *68*, 1507-1518.
29. T. Laube; J. D. Dunitz; D. Seebach *Helv. Chim. Acta* **1985**, *68*, 1373-1393.
30. M. B. Eleveld; H. Hogeveen *Tetrahedron Lett.* **1986**, *27*, 631-634.
31. E. Juaristi; A. K. Beck; J. Hansen; T. Matt; T. Mukhopadhyay; M. Simson; D. Seebach *Synthesis* **1993**, 1271-1290.
32. E. Vedejs; N. Lee *J. Am. Chem. Soc.* **1995**, *117*, 891-900.
33. D. B. Collum *Acc. Chem. Res.* **1992**, *25*, 448-454.
34. H. B. McCall; R. C. S. Williams In *Comprehensive Organic Synthesis*; S. Patai, Ed.; Pergamon: Oxford, 1991; Vol. 3, p 1-63.



49. I. Fleming *Frontier Orbitals and Organic Chemical Reactions*; Wiley-Interscience: New York, 1976.
50. C. Agami *Tetrahedron Lett.* **1977**, 2801-2804.
51. C. Agami; M. Chauvin; J. Levisalles *Tetrahedron Lett.* **1979**, 1855-1858.
52. C. Agami; J. Levisalles; B. L. Cicero *Tetrahedron* **1979**, 35, 961-967.
53. K. N. Houk; M. N. Paddon-Row *J. Am. Chem. Soc.* **1986**, 108, 2659-2962.
54. N. G. Rondan; M. N. Paddon-Row; P. Caramella; K. N. Houk *J. Am. Chem. Soc.* **1981**, 103, 2436-2438.
55. K. N. Houk *Pure Appl. Chem.* **1983**, 55, 277-282.
56. D. Seebach; J. Zimmerman; U. Gysel; R. Ziegler; T.-K. Ha *J. Am. Chem. Soc.* **1988**, 110, 4763-4772.
57. H. O. House; B. A. Tefertiller; H. D. Olmstead *J. Org. Chem.* **1968**, 33, 935-942.
58. I. Kuwajima; E. Nakamura; M. Shimizu *J. Am. Chem. Soc.* **1982**, 104, 1025-1030.
59. R. W. Hoffmann *Chem. Rev.* **1989**, 89, 1841-1860.
60. P. Caramella; N. G. Rondan; M. N. Paddon-Row; K. N. Houk *J. Am. Chem. Soc.* **1981**, 103, 2438-2440.
61. G. J. McGarvey; J. M. Williams *J. Am. Chem. Soc.* **1985**, 107, 1435-1437.
62. D. Seebach; R. Naef; G. Calderari *Tetrahedron* **1984**, 40, 1313-1324.
63. R. Fitzi; D. Seebach *Tetrahedron* **1988**, 44, 5277-5292.
64. D. Seebach; A. Fadel *Helv. Chim. Acta* **1985**, 68, 1243-1250.
65. D. Seebach; J. D. Aebi; R. Naef; T. Weber *Helv. Chim. Acta* **1985**, 68, 144-154.
66. D. Seebach; B. Lamatsch; R. Amstutz; A. K. Beck; M. Dobler; M. Egli; R. Fitzi; M. Gautschi; B. Herradón; P. C. Hidber; J. J. Irwin; R. Locher; M. Maestro; T. Maetzke; A. Mouriño; E. Pfammatter; D. A. Plattner; C. Schickli; W. B. Schweizer; P. Seiler; G. Stucky; W. Petter; J. Escalante; E. Juaristi; D. Quintana; C. Miravittles; E. Molins *Helv. Chim. Acta* **1992**, 75, 913-934.
67. E. Vedejs; S. C. Fields; M. R. Schrimpf *J. Am. Chem. Soc.* **1993**, 115, 11612-11613.
68. R. Downham; K. S. Kim; S. V. Ley; M. Woods *Tetrahedron Lett.* **1994**, 35, 769-772.
69. G.-J. Boons; R. Downham; K. S. Kim; S. V. Ley; M. Woods *Tetrahedron* **1994**, 50.
70. U. Schöllkopf *Tetrahedron* **1983**, 39, 2085-2091.
71. R. M. Williams; M.-N. Im *J. Am. Chem. Soc.* **1991**, 113, 9276-9286.
72. S. Yamada; T. Oguri; T. Shioiri *J. Chem. Soc.* **1976**, 136-137.
73. E. Ade; G. Helmchen; G. Heiligenmann *Tetrahedron Lett.* **1980**, 21, 1137-1140.
74. R. Schmierer; G. Grote-meier; G. Helmchen; A. Selim *Angew. Chem. Int. Ed. Engl.* **1981**, 20, 207-208.
75. G. Helmchen; A. Selim; D. Dorsch; I. Taufer *Tetrahedron Lett.* **1983**, 24, 3213-3216.
76. G. Helmchen; R. Schmierer *Tetrahedron Lett.* **1983**, 24, 1235-1238.
77. A. I. Meyers; E. D. Mihelich *Angew. Chem. Int. Ed. Engl.* **1976**, 15, 270-281.
78. A. I. Meyers *Acc. Chem. Res.* **1978**, 11, 375-381.
79. K. A. Lutomski; A. I. Meyers In *Asymmetric Synthesis*; J. D. Morrison, Ed.; Academic: Orlando, 1984; Vol. 3, p 213-273.
80. P. E. Sonnet; R. R. Heath *J. Org. Chem.* **1980**, 45, 3137-3139.
81. D. A. Evans; J. M. Takacs *Tetrahedron Lett.* **1980**, 21, 4233-4236.
82. D. A. Evans; J. M. Takacs; L. R. McGee; M. D. Ennis; D. J. Mathre; J. Bartroli *Pure Appl. Chem.* **1981**, 53, 1109-1127.
83. D. A. Evans; M. D. Ennis; D. J. Mathre *J. Am. Chem. Soc.* **1982**, 104, 1737-1739.
84. J. R. Gage; D. A. Evans *Organic Syntheses* **1993**, Coll. Vol. VIII, 339-343.
85. D. A. Evans; T. C. Britton; J. A. Ellman *Tetrahedron Lett.* **1987**, 28, 6141-6144.
86. D. A. Evans; J. Bartroli *Tetrahedron Lett.* **1982**, 23, 807-810.
87. D. A. Evans; R. L. Dow; T. L. Shih; J. M. Takacs; R. Zahler *J. Am. Chem. Soc.* **1990**, 112, 5290-5313.
88. W. Oppolzer; R. Moretti; S. Thomi *Tetrahedron Lett.* **1989**, 30, 5603-5606.

89. B. H. Kim; D. P. Curran *Tetrahedron* **1993**, *49*, 293-318.
90. A. I. Meyers; M. Harre; R. Garland *J. Am. Chem. Soc.* **1984**, *106*, 1146-1148.
91. A. I. Meyers; B. A. Lefker; T. J. Sowin; L. J. Westrum *J. Org. Chem.* **1989**, *54*, 4243-4246.
92. A. I. Meyers; K. T. Wanner *Tetrahedron Lett.* **1985**, *26*, 2047-2050.
93. A. I. Meyers; B. A. Lefker; K. T. Wanner; R. A. Aitken *J. Org. Chem.* **1986**, *51*, 1936-1938.
94. A. I. Meyers; B. A. Lefker *Tetrahedron* **1987**, *43*, 5663-5676.
95. A. I. Meyers; D. Berney *Organic Syntheses* **1990**, *69*, 55-65.
96. D. Romo; A. I. Meyers *Tetrahedron* **1991**, *47*, 9503-9569.
97. A. I. Meyers; L. J. Westrum *Tetrahedron Lett.* **1993**, *34*, 7701-7704.
98. L. Snyder; A. I. Meyers *J. Org. Chem.* **1993**, *58*, 7507-7515.
99. A. I. Meyers; R. H. Wallace *J. Org. Chem.* **1989**, *54*, 2509-2510.
100. A. I. Meyers; B. A. Lefker *J. Org. Chem.* **1986**, *51*, 1541-1544.
101. A. I. Meyers; R. Hanreich; K. T. Wanner *J. Am. Chem. Soc.* **1985**, *107*, 7776-7778.
102. A. I. Meyers; M. A. Stuyers *Tetrahedron Lett.* **1989**, *30*, 1741-1744.
103. A. I. Meyers; D. Berney *J. Org. Chem.* **1989**, *54*, 4673-4676.
104. D. Enders In *Asymmetric Synthesis*; J. D. Morrison, Ed.; Academic: Orlando, 1984; Vol. 3, p 275-339.
105. D. Enders; H. Kipphardt; P. Fey *Organic Syntheses* **1987**, *65*, 183-202.
106. D. E. Bergbreiter; M. Momongan In *Comprehensive Organic Synthesis. Selectivity, Strategy, and Efficiency in Modern Organic Chemistry*; B. M. Trost, I. Fleming, Eds.; Pergamon: Oxford, 1991; Vol. 2, p 503-526.
107. D. Enders In *Stereoselective Synthesis: Lectures Honouring Prof. Dr. h. c. Rudolf Wiechert*; E. Ottow, K. Schöllkopf, B. G. Schulz, Eds.; Springer: Berlin, 1994, p 63-90.
108. E. J. Corey; D. Enders *Tetrahedron Lett.* **1976**, 3-6.
109. E. J. Corey; D. Enders *Chem. Ber.* **1978**, *111*, 1337-1361.
110. D. Enders; P. Fey; H. Kipphardt *Organic Syntheses* **1987**, *65*, 173-182.
111. D. Enders; H. Eichenauer *Chem. Ber.* **1979**, *112*, 2933-2960.
112. D. Enders; H. Eichenauer; U. Baus; H. Schubert; K. A. M. Kremer *Tetrahedron* **1984**, *40*, 1345-1359.
113. D. Enders; V. Bhushan Z. *Naturforsch.* **1987**, *42*, 1595-1596.
114. D. Enders; A. Plant *Synlett* **1990**, 725-726.
115. R. E. Gawley; E. J. Termine *Synth. Commun.* **1982**, *12*, 15-18.
116. D. Enders; H. Dyker; G. Raabe *Angew. Chem. Int. Ed. Engl.* **1992**, *31*, 618-620.
117. K. G. Davenport; H. Eichenauer; D. Enders; M. Newcomb; D. E. Bergbreiter *J. Am. Chem. Soc.* **1979**, *101*, 5654-5659.
118. D. Enders *Chem. Scripta* **1985**, *25*, 139-147.
119. D. Enders; G. Bachstädter; K. A. M. Kremer; M. Marsch; K. Harms; G. Boche *Angew. Chem. Int. Ed. Engl.* **1988**, *27*, 1522-1524.
120. K. Mori; H. Nomii; T. Chuman; M. Kohno; K. Kato; M. Noguchi *Tetrahedron* **1982**, *38*, 3705-3711.
121. K. C. Nicolaou; D. P. Papahatjis; D. A. Claremon; R. E. Dolle, III *J. Am. Chem. Soc.* **1981**, *103*, 6967-6969.
122. H. Hogeveen; L. Zwart *Tetrahedron Lett.* **1982**, *23*, 105-108.
123. C. M. Cain; N. S. Simpkins *Tetrahedron Lett.* **1987**, *28*, 3723-3724.
124. R. Shirai; M. Tanaka; K. Koga *J. Am. Chem. Soc.* **1986**, *108*, 543-545.
125. D. Sato; H. Kawasaki; I. Shimada; Y. Arata; K. Okamura; T. Date; K. Koga *J. Am. Chem. Soc.* **1992**, *114*, 761-763.
126. R. P. C. Cousins; N. S. Simpkins *Tetrahedron Lett.* **1989**, *30*, 7241-7244.
127. K. Aoki; H. Noguchi; K. Tomioka; K. Koga *Tetrahedron Lett.* **1993**, *34*, 5105-5108.
128. K. Koga *Pure Appl. Chem.* **1994**, *66*, 1487-1492.
129. J. K. Whitesell; S. W. Felman *J. Org. Chem.* **1980**, *45*.
130. H. Kim; H. Kawasaki; M. Nakajima; K. Koga *Tetrahedron Lett.* **1989**, *30*, 6537-6540.

131. M. Sobukawa; K. Koga *Tetrahedron Lett.* **1993**, 34, 5101-5104.
132. E. Vedejs; N. Lee *J. Am. Chem. Soc.* **1991**, 113, 5483-5485.
133. S. Hünig In *Stereoselective Synthesis*; G. Helmchen, R. W. Hoffmann, J. Mulzer, E. Schaumann, Eds.; Georg Thieme: Stuttgart, 1995; Vol. E21d, p Chapter 2.1.
134. I. T. Barnish; M. Corless; P. J. Dunn; D. Ellis; P. W. Finn; J. D. Hardstone; K. James *Tetrahedron Lett.* **1993**, 34, 1323-1326.
135. K. Fujii; K. Tanaka; H. Miyamoto *Tetrahedron Asymmetry* **1993**, 4, 247-249.
136. C. Fehr; O. Guntern *Helv. Chim. Acta* **1992**, 75, 1023-1028.
137. C. Fehr; I. Stempf; J. Galindo *Angew. Chem. Int. Ed. Engl.* **1993**, 32, 1042-1044.
138. C. Fehr; I. Stempf; J. Galindo *Angew. Chem. Int. Ed. Engl.* **1993**, 32, 1044-1046.
139. A. Yanagisawa; T. Kurabayashi; T. Kikuchi; H. Yamamoto *Angew. Chem. Int. Ed., Engl.* **1994**, 33, 107-109.
140. E. Vedejs; N. Lee; S. T. Sakata *J. Am. Chem. Soc.* **1994**, 116, 2175-2176.
141. T. Yamashita; H. Mitsui; W. H; N. Nakamura *Bull. Chem. Soc. Jpn.* **1982**, 55, 961-962.
142. H. Hogeveen; W. M. P. B. Menge *Tetrahedron Lett.* **1986**, 27, 2767-2770.
143. A. Ando; T. Shiori *J. Chem. Soc., Chem. Commun.* **1987**, 656-658.
144. D. Seebach; D. Wasmuth *Angew. Chem. Int. Ed. Engl.* **1981**, 20, 971.
145. T. Kawabata; K. Yahiro; K. Fujii *J. Am. Chem. Soc.* **1991**, 113, 9694-9696.
146. T. Kawabata; T. Wirth; K. Yahiro; H. Suzuki; K. Fujii *J. Am. Chem. Soc.* **1994**, 116, 10809-10810.
147. K. Tomioka; M. Shindo; K. Koga *Chem. Pharm. Bull.* **1989**, 37, 1120-1122.
148. M. Murakata; M. Nakajima; K. Koga *J. Chem. Soc., Chem. Commun.* **1990**, 1657-1658.
149. M. Imai; A. Hagihara; H. Kawasaki; K. Manabe; K. Koga *J. Am. Chem. Soc.* **1994**, 116, 8829-8830.
150. D. L. Hughes; U.-H. Dolling; K. M. Ryan; E. F. Schoenewaldt; E. J. J. Grabowski *J. Org. Chem.* **1987**, 52, 4745-4752.
151. M. J. O'Donnell; W. D. Bennett; S. Wu *J. Am. Chem. Soc.* **1989**, 111, 2353-2355.
152. F. Mohamadi; N. G. J. Richards; W. C. Guida; R. Liskamp; M. Lipton; C. Caufield; G. Chang; T. Hendrickson; W. C. Still *J. Comput. Chem.* **1990**, 11, 440-467.
153. H. J. Reich; M. A. Medina; M. D. Bowe *J. Am. Chem. Soc.* **1992**, 114, 11003-11004.
154. P. Beak; H. Du *J. Am. Chem. Soc.* **1993**, 115, 2516-2518.
155. S. Thayumanavan; S. Lee; C. Liu; P. Beak *J. Am. Chem. Soc.* **1994**, 116, 9755-9756.
156. A. Krief *Tetrahedron* **1980**, 36, 2531-2640.
157. N. G. Rondan; K. N. Houk; P. Beak; W. J. Zajdel; J. Chandrasekhar; P. v. R. Schleyer *J. Org. Chem.* **1981**, 46, 4108-4110.
158. R. D. Bach; M. L. Braden; G. J. Wolber *J. Org. Chem.* **1983**, 48, 1509-1514.
159. L. J. Bartolotti; R. E. Gawley *J. Org. Chem.* **1989**, 54, 2980-2982.
160. D. Seebach; J. Hansen; P. Seiler; J. M. Gromek *J. Organomet. Chem.* **1985**, 285, 1-13.
161. G. Boche; M. Marsch; J. Harbach; K. Harms; B. Ledig; F. Schubert; J. C. W. Lohrenz; H. Albrecht *Chem. Ber.* **1993**, 126, 1887-1894.
162. P. v. R. Schleyer; T. Clark; A. J. Kos; G. W. Spitznagel; C. Rohde; D. Arad; K. N. Houk; N. G. Rondan *J. Am. Chem. Soc.* **1984**, 106, 6467-6475.
163. R. E. Gawley; Q. Zhang *Tetrahedron* **1994**, 50, 6077-6088.
164. D. R. Cheshire In *Comprehensive Organic Synthesis. Selectivity, Strategy, and Efficiency in Modern Organic Chemistry*; B. M. Trost, I. Fleming, Eds.; Pergamon: Oxford, 1991; Vol. 3, p 193-205.
165. W. C. Still; C. Sreekumar *J. Am. Chem. Soc.* **1980**, 102, 1201-1202.
166. J.-M. Lehn; G. Wipff *J. Am. Chem. Soc.* **1976**, 98, 7498-7505.
167. J. S. Sawyer; A. Kucerovy; T. L. Macdonald; G. J. McGarvey *J. Am. Chem. Soc.* **1988**, 110, 842-853.
168. H. J. Reich; J. P. Borst; M. B. Coplein; N. H. Phillips *J. Am. Chem. Soc.* **1992**, 114, 6577-6579.

169. J. A. Marshall; W. Y. Gung *Tetrahedron Lett.* **1988**, 29, 1657-1660.
170. P. C.-M. Chan; J. M. Chong *J. Org. Chem.* **1988**, 53, 5584-5586.
171. J. A. Marshall; G. S. Welmaker; B. W. Gung *J. Am. Chem. Soc.* **1991**, 113, 647-656.
172. J. M. Chong; E. K. Mar *Tetrahedron Lett.* **1991**, 32, 5683-5686.
173. D. S. Matteson; P. B. Tripathy; A. Sarkur; K. N. Sadhu *J. Am. Chem. Soc.* **1989**, 111, 4399-4402.
174. M. H. Abraham In *Comprehensive Chemical Kinetics*; C. H. Bamford, C. F. H. Tinner, Eds.

- 209. R. E. Gawley; G. A. Smith *Tetrahedron Lett.* **1988**, 29, 301-302.
- 210. P. Beak; S. T. Kerrick; S. Wu; J. Chu *J. Am. Chem. Soc.* **1994**, 116, 3231-3239.
- 211. D. J. Gallagher; S. T. Kerrick; P. Beak *J. Am. Chem. Soc.* **1992**, 114, 5872-5873.
- 212. D. J. Gallagher; P. Beak *J. Org. Chem.* **1995**, 60, 7092-7093.
- 213. R. E. Gawley; Q. Zhang *J. Am. Chem. Soc.* **1993**, 115, 7515-7516.
- 214. A. I. Meyers; P. D. Edwards; W. F. Reiker; T. R. Bailey *J. Am. Chem. Soc.* **1984**, 106, 3270-3276.
- 215. P. Beak; W.-K. Lee *Tetrahedron Lett.* **1989**, 30, 1197-1200.
- 216. P. Beak; W. K. Lee *J. Org. Chem.* **1993**, 58, 1109-1117.
- 217. R. E. Gawley; Q. Zhang *J. Org. Chem.* **1995**, 60, 5763-5769.